

Hydrodynamics vs perturbative QCD mechanism in production of hadrons in heavy ion collisions

Jan Nemchik

Czech Technical University in Prague, FNSPE, Prague, Czech Republic
Institute of Experimental Physics SAS, Košice, Slovakia

The 15th conference on Elastic and Diffractive scattering 2013
September 9-13, 2013, Saariselka, Finland

In collaboration with
Boris Kopeliovich, & Irina Potashnikova

Outline

pQCD mechanism - nuclear suppression at large p_T

- Introduction \Rightarrow p_T - behavior of nuclear suppression observed at RHIC and LHC

Outline

pQCD mechanism - nuclear suppression at large p_T

- Introduction \Rightarrow p_T - behavior of nuclear suppression observed at RHIC and LHC
- Final state interaction (FSI) \Rightarrow attenuation of a small size dipole in a medium

Outline

pQCD mechanism - nuclear suppression at large p_T

- Introduction \Rightarrow p_T - behavior of nuclear suppression observed at RHIC and LHC
- Final state interaction (FSI) \Rightarrow attenuation of a small size dipole in a medium
- Initial state interaction (ISI) \Rightarrow energy conservation constraints

Outline

pQCD mechanism - nuclear suppression at large p_T

- Introduction \Rightarrow p_T - behavior of nuclear suppression observed at RHIC and LHC
- Final state interaction (FSI) \Rightarrow attenuation of a small size dipole in a medium
- Initial state interaction (ISI) \Rightarrow energy conservation constraints
- Numerical results vs data
 - \Rightarrow comparison with LHC data
 - \Rightarrow comparison with RHIC data

Interplay of the pQCD mech. and hydrodynamics - small- p_T suppression

Outline

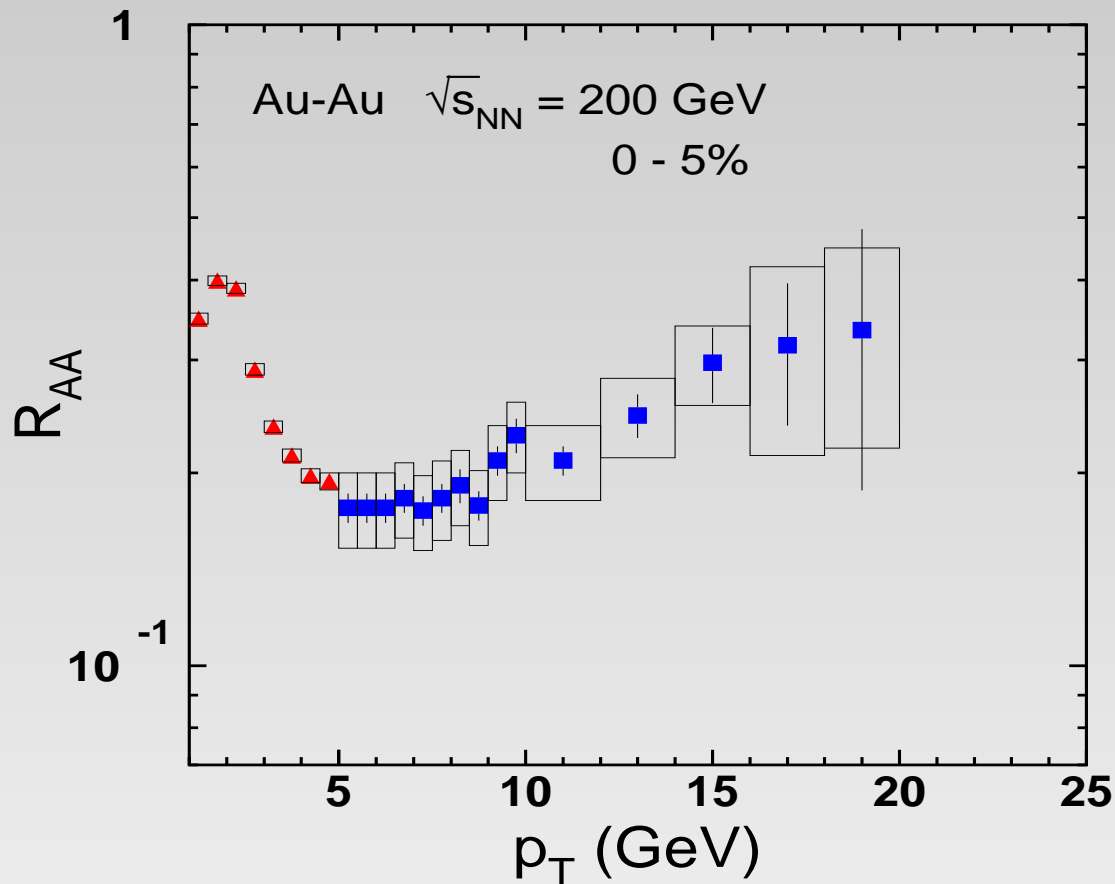
pQCD mechanism - nuclear suppression at large p_T

- Introduction \Rightarrow p_T - behavior of nuclear suppression observed at RHIC and LHC
- Final state interaction (FSI) \Rightarrow attenuation of a small size dipole in a medium
- Initial state interaction (ISI) \Rightarrow energy conservation constraints
- Numerical results vs data
 - \Rightarrow comparison with LHC data
 - \Rightarrow comparison with RHIC data

Interplay of the pQCD mech. and hydrodynamics - small- p_T suppression

- Summary & Outlook

High- p_T hadrons at RHIC

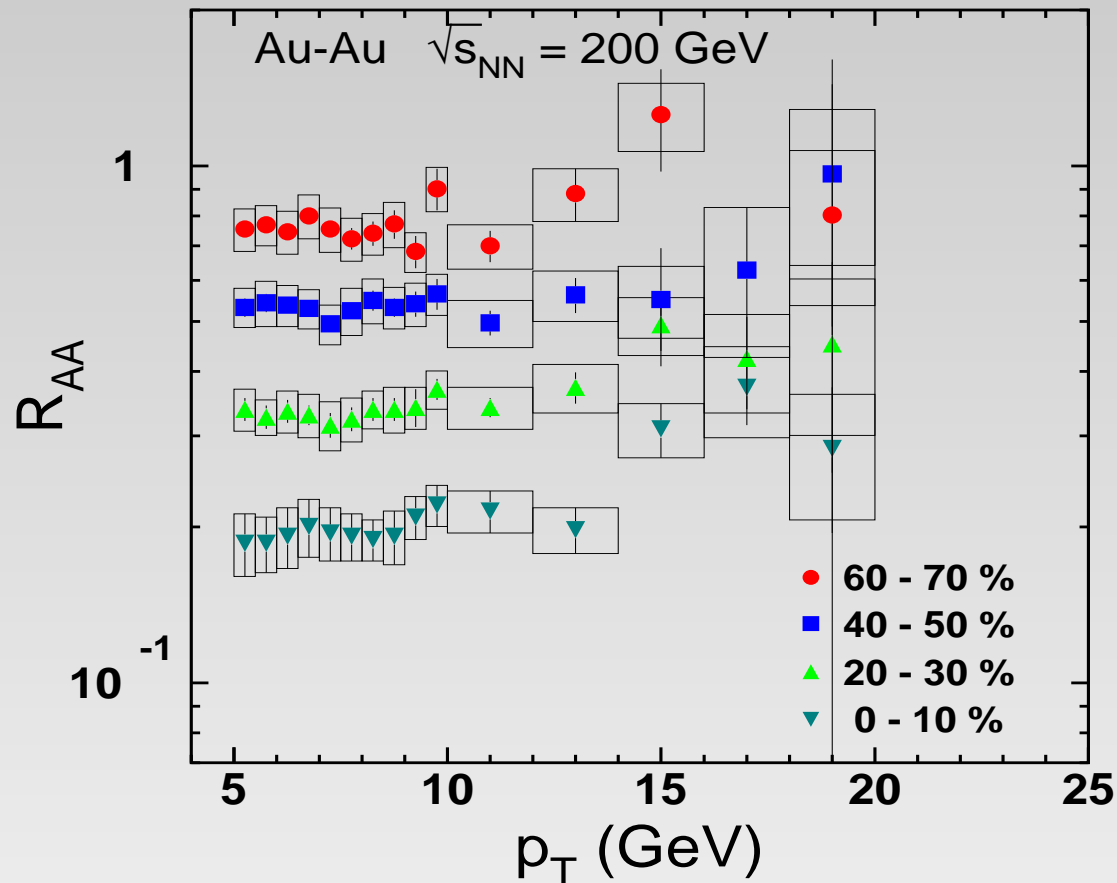


Nuclear attenuation factor $R_{AA}(p_T)$ as function of p_T for neutral pions produced in central, 0-5%, gold-gold collisions at $\sqrt{s} = 200$ GeV.

[TRIANGLES - PHENIX Collaboration, A. Adare et al.; Phys. Rev. Lett. **101**, 232301 (2008).]

[SQUARES - PHENIX Collaboration, M. L. Porschke et al.; J. Phys. G **38**, 124016 (2011).]

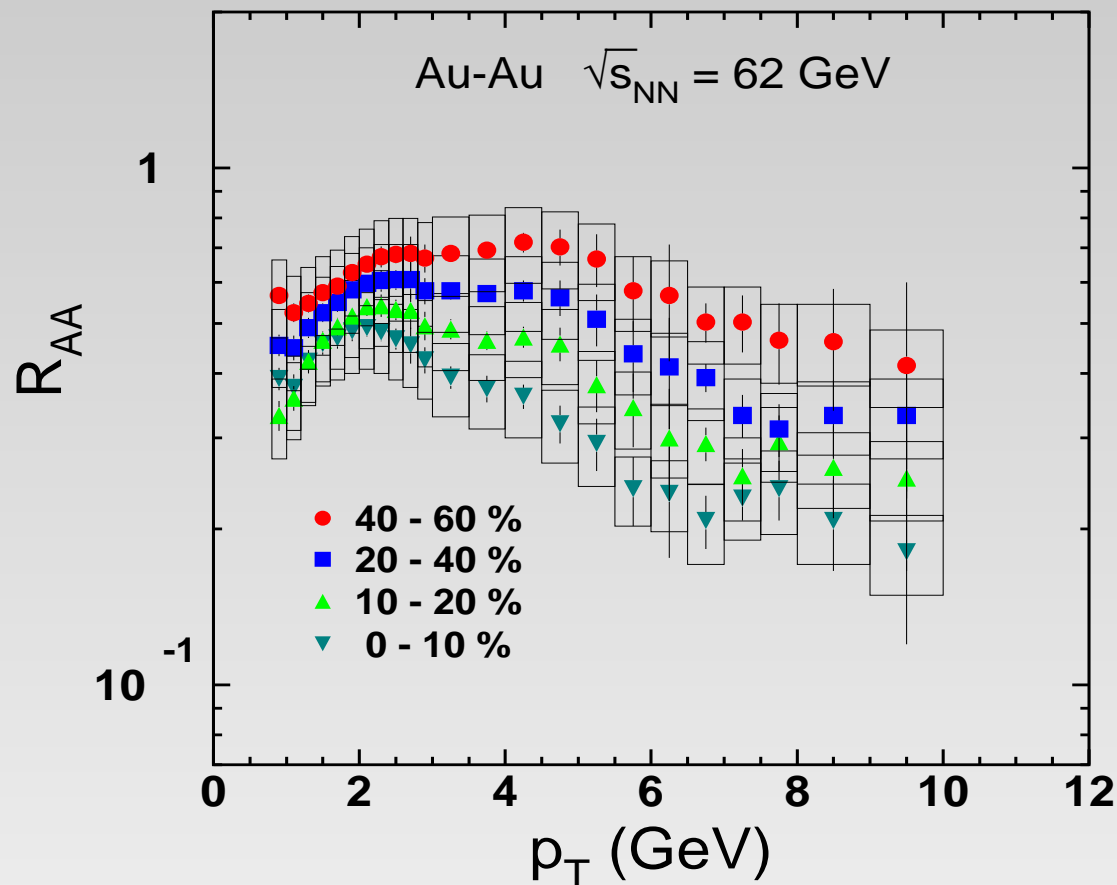
High- p_T hadrons at RHIC



Nuclear attenuation factor $R_{AA}(p_T)$ as function of p_T for neutral pions produced in gold-gold collisions at $\sqrt{s} = 200$ GeV and at centralities 0-10%, 20-30%, 40-50%, 60-70%.

[PHENIX Collaboration, A. Adare et al., Phys. Rev. C87, 034911 (2013).]

High- p_T hadrons at RHIC

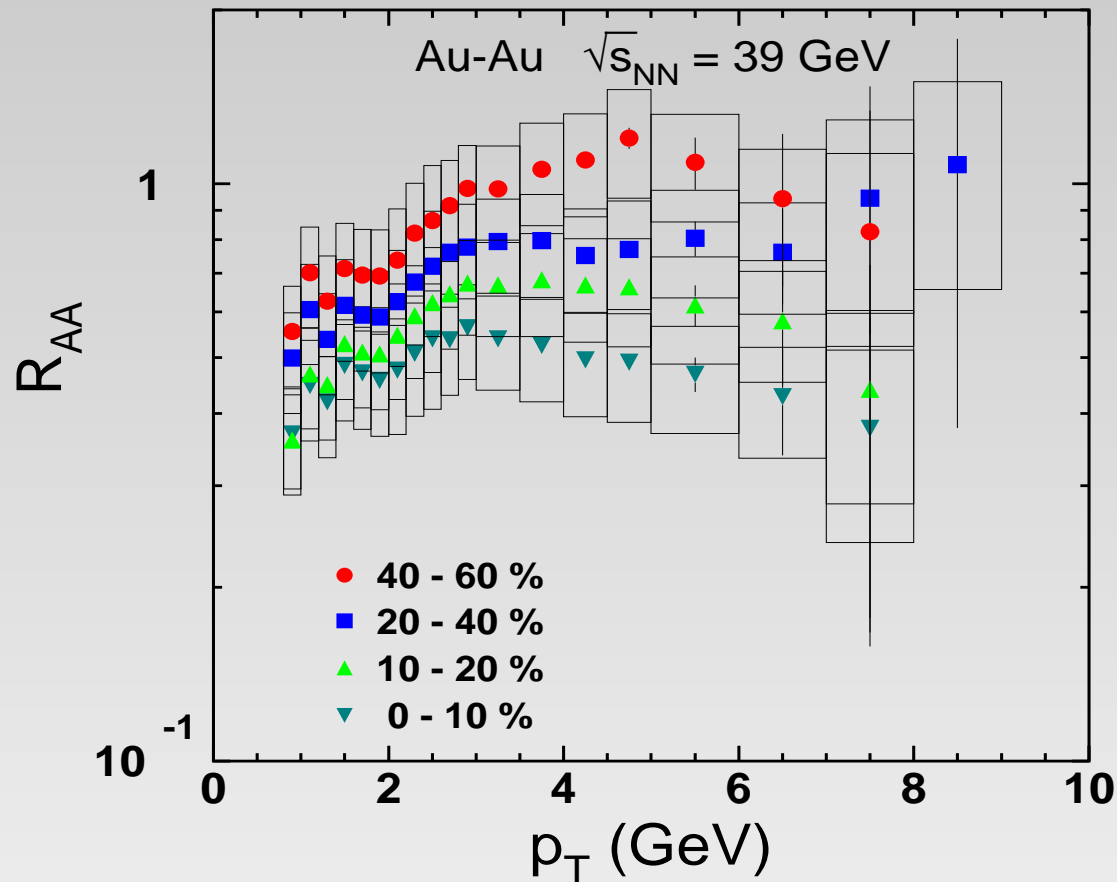


Nuclear attenuation factor $R_{AA}(p_T)$ as function of p_T for neutral pions produced in gold-gold collisions at $\sqrt{s} = 62$ GeV and at centralities 0-10%, 10-20%, 20-40%, 40-60%.

[PHENIX Collaboration, [http :](http://www.phenix.bnl.gov/WWW/plots/show_plot.php?editkey=p1118)

[//www.phenix.bnl.gov/WWW/plots/show_plot.php?editkey = p1118](http://www.phenix.bnl.gov/WWW/plots/show_plot.php?editkey=p1118)].

High- p_T hadrons at RHIC

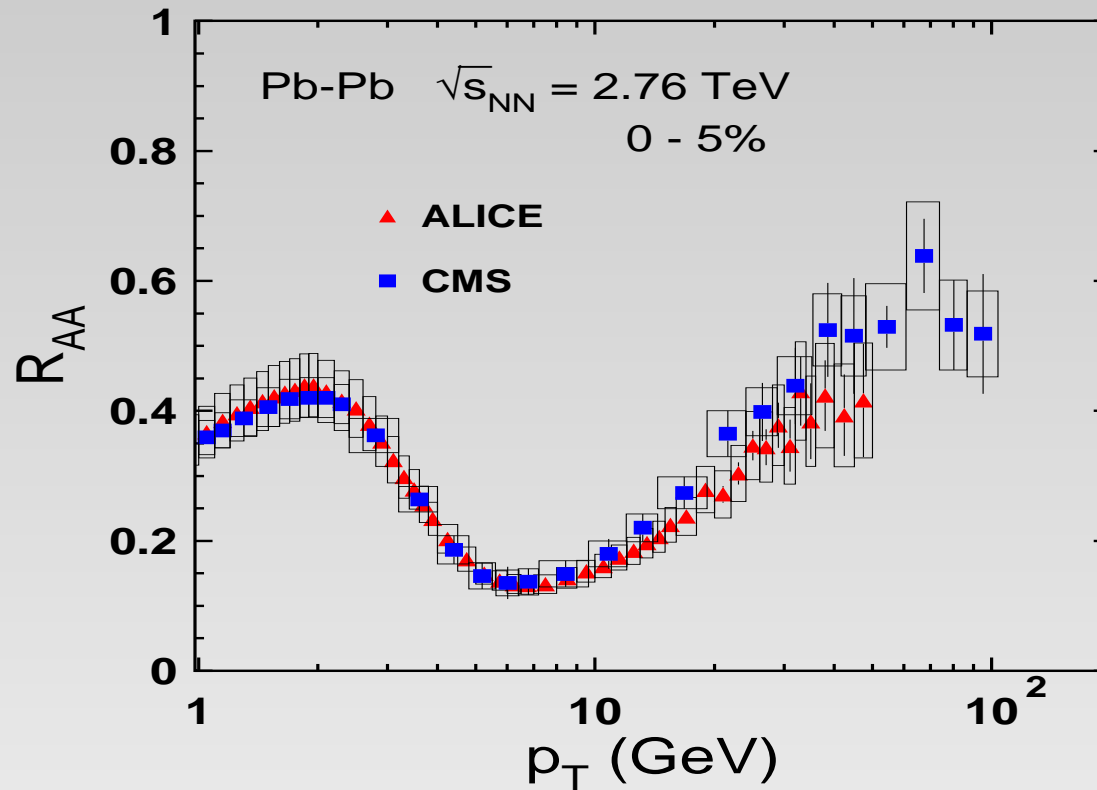


Nuclear attenuation factor $R_{AA}(p_T)$ as function of p_T for neutral pions produced in gold-gold collisions at $\sqrt{s} = 39$ GeV and at centralities 0-10%, 10-20%, 20-40%, 40-60%.

[PHENIX Collaboration, [http :](http://www.phenix.bnl.gov/WWW/plots/show_plot.php?editkey=p1117)

[//www.phenix.bnl.gov/WWW/plots/show_plot.php?editkey = p1117](http://www.phenix.bnl.gov/WWW/plots/show_plot.php?editkey=p1117)].

High- p_T hadrons at LHC



Nuclear attenuation factor $R_{AA}(p_T)$ as function of p_T for charged hadrons produced in central, 0-5%, lead-lead collisions at $\sqrt{s} = 2.76$ TeV.

[TRIANGLES - ALICE Collaboration, B. Abelev et al.; Phys. Lett. B **720**, 52 (2013); J. Otwinowski et al.; J. Phys. G **38**, 124112 (2011).]

[SQUARES - CMS Collaboration, Y.-J. Lee et al.; J. Phys. G **38**, 124015 (2011). A. S. Yoon et al.; J. Phys. G **38**, 124116 (2011).]

LHC vs. RHIC data

- LHC data expose novel features in comparison with measurements at RHIC

LHC vs. RHIC data

- LHC data expose novel features in comparison with measurements at RHIC
- the nuclear suppression factor R_{AA} reaches significantly smaller values \Rightarrow at the LHC energies hadrons originate mainly from fragmentation of gluons with larger color charge than quarks dominating at RHIC and **gluons dissipate energy with a higher rate** \Leftarrow FSI

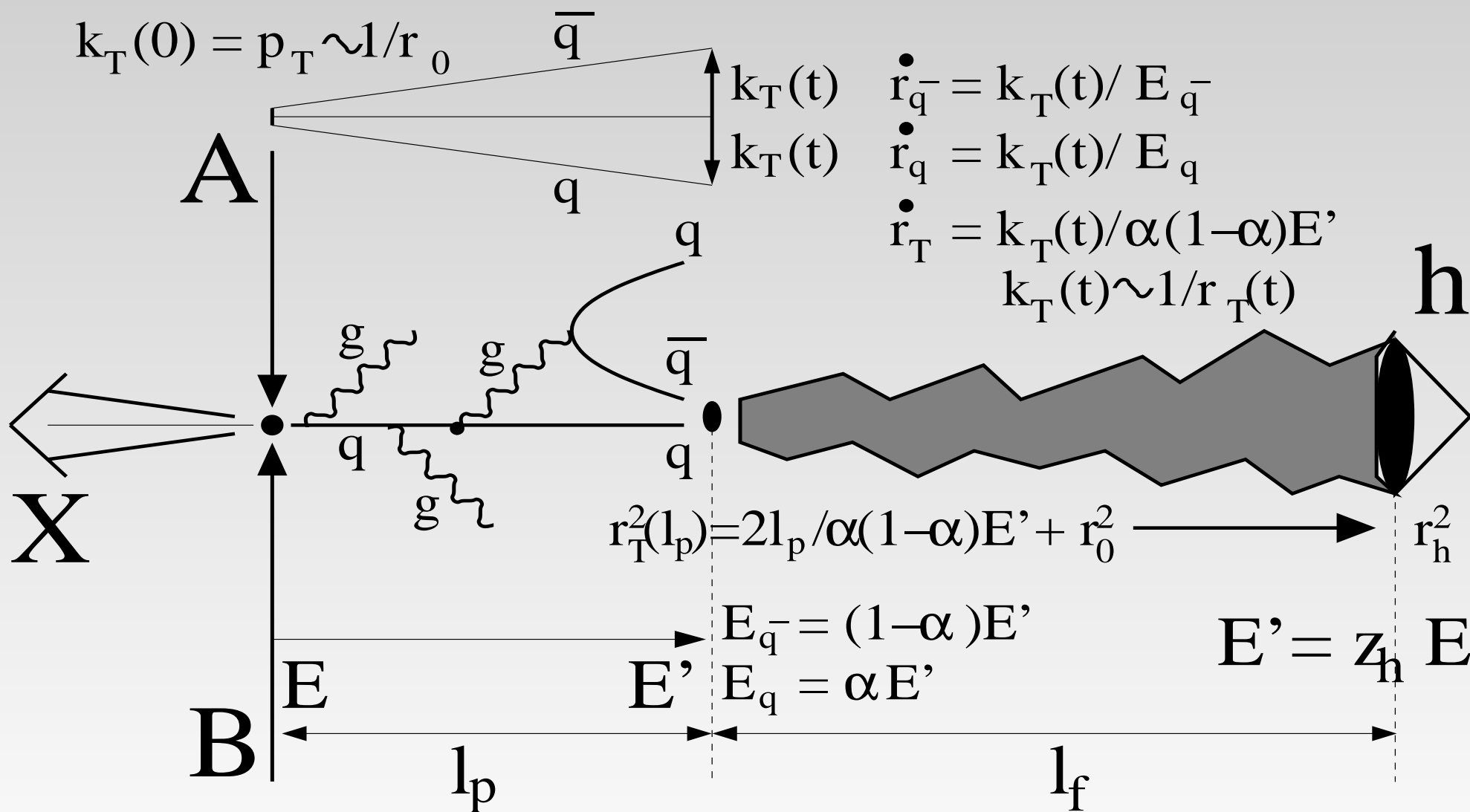
LHC vs. RHIC data

- LHC data expose novel features in comparison with measurements at RHIC
- the nuclear suppression factor R_{AA} reaches significantly smaller values \Rightarrow at the LHC energies hadrons originate mainly from fragmentation of gluons with larger color charge than quarks dominating at RHIC and **gluons dissipate energy with a higher rate** \Leftarrow FSI
- R_{AA} steeply rises with p_T at LHC but exposes rather flat p_T -behavior at RHIC \Rightarrow it is affected by restrictions imposed by energy conservation \Leftarrow ISI

Final state interaction

$$y = 0 : E = Q = k_T = p_T / z_h$$

$$k_T(0) = p_T \sim 1/r_0$$



$$\langle l_p \rangle \propto k_T(1-z_h)/Q^2 \quad \text{hand icon} \quad l_f \propto 2E' / (m_h^2 - m_h^2)$$

Final state interaction

Ingredients for calculation of suppression

- time- dependent transport coefficient $\hat{q}(t)$

⇒ survival probability for $\bar{q}q$ dipole propagating through a medium

Final state interaction

Ingredients for calculation of suppression

- time- dependent transport coefficient $\hat{q}(t)$
- transverse size $r_T(t)$ - evolution of a $\bar{q}q$ dipole

⇒ survival probability for $\bar{q}q$ dipole propagating through a medium

Final state interaction

Ingredients for calculation of suppression

- time- dependent **transport coefficient** $\hat{q}(t)$
- **transverse size** $r_T(t)$ - evolution of a $\bar{q}q$ dipole
- model for hadronization: $\langle l_p \rangle \propto \tilde{E}(1 - z_h) / \langle \kappa(Q^2) \rangle$
 - \Rightarrow several effects acting in opposite directions:
 - the Lorentz factor makes l_p **LONGER** with energy
 - the increasing virtuality gives rise to a more intensive gluon radiation and E-loss in vacuum, leading to **SHORTER** l_p
 - the Sudakov suppression , essential at large z_h , also **SHORTENS** l_p

\Rightarrow survival probability for $\bar{q}q$ dipole propagating through a medium

Final state interaction

Transport coefficient

- FSI contribution to nuclear suppression is related to properties of created medium.

Final state interaction

Transport coefficient

- FSI contribution to nuclear suppression is related to properties of created medium.
- Such medium is described in terms of transport coefficient \hat{q} - the magnitude of broadening experienced by a parton through a path length 1 fm in the medium

Final state interaction

Transport coefficient

- FSI contribution to nuclear suppression is related to properties of created medium.
- Such medium is described in terms of transport coefficient \hat{q} - the magnitude of broadening experienced by a parton through a path length 1 fm in the medium
- We rely on the usual assumption - initial medium density at time $t = t_0$ is proportional to the number of participants n_{part} and density is diluting with time as $1/t$

Final state interaction

Transport coefficient

- FSI contribution to nuclear suppression is related to properties of created medium.
- Such medium is described in terms of transport coefficient \hat{q} - the magnitude of broadening experienced by a parton through a path length 1 fm in the medium
- We rely on the usual assumption - initial medium density at time $t = t_0$ is proportional to the number of participants n_{part} and density is diluting with time as $1/t$
- Then the time dependent transport coefficient reads:

$$\hat{q}(t, \vec{b}, \vec{\tau}) = \frac{\hat{q}_0 t_0}{t} \frac{n_{part}(\vec{b}, \vec{\tau})}{n_{part}(0, 0)},$$

Final state interaction

Transport coefficient

- the parameter \hat{q}_0 represents the maximal value of \hat{q} , for the medium produced at $t = t_0$ in central collision at $b = \tau = 0$

Final state interaction

Transport coefficient

- the parameter \hat{q}_0 represents the maximal value of \hat{q} , for the medium produced at $t = t_0$ in central collision at $b = \tau = 0$
- variable \vec{b} - impact parameter of collision
- variable $\vec{\tau}$ - impact parameter of position of the parton

FSI: attenuation of a dipole

$r_T(t)$ - evolution of a $\bar{q}q$ dipole

- during production time l_p a $\bar{q}q$ dipole is created

FSI: attenuation of a dipole

$r_T(t)$ - evolution of a $\bar{q}q$ dipole

- during production time l_p a $\bar{q}q$ dipole is created
- this dipole propagating in a medium attenuates with the cross section $\propto r_T^2$, where r_T^2 is rising with time.

FSI: attenuation of a dipole

$r_T(t)$ - evolution of a $\bar{q}q$ dipole

- during production time l_p a $\bar{q}q$ dipole is created
- this dipole propagating in a medium attenuates with the cross section $\propto r_T^2$, where r_T^2 is rising with time.
- at low energies - dipole quickly expands to the hadronic size
at high energies - Lorentz time dilation freezes the initial small size of the dipole for the time of propagation
 \Rightarrow the medium becomes more transparent with rising energy of the dipole, \tilde{E}

FSI: attenuation of a dipole

$r_T(t)$ - evolution of a $\bar{q}q$ dipole

- during production time l_p a $\bar{q}q$ dipole is created
- this dipole propagating in a medium attenuates with the cross section $\propto r_T^2$, where r_T^2 is rising with time.
- at low energies - dipole quickly expands to the hadronic size
at high energies - Lorentz time dilation freezes the initial small size of the dipole for the time of propagation
 \Rightarrow the medium becomes more transparent with rising energy of the dipole, \tilde{E}
- the transverse expansion of a $\bar{q}q$ dipole reads:

$$\frac{dr_T}{dt} = \frac{k_T(t)}{\alpha(1 - \alpha) \tilde{E}}$$

α - fractional light-cone momentum of the parton.

[B.Z. Kopeliovich, J. Nemchik; J. Phys. G38, 043101 (2011)]

FSI: attenuation of a dipole

$r_T(t)$ - evolution of a $\bar{q}q$ dipole

- applying the uncertainty relation $k_T(t) \sim 1/r_T$, we get,

$$r_T^2(t) = \frac{2t}{\alpha(1-\alpha)\tilde{E}} + r_0^2,$$

FSI: attenuation of a dipole

$r_T(t)$ - evolution of a $\bar{q}q$ dipole

- applying the uncertainty relation $k_T(t) \sim 1/r_T$, we get,

$$r_T^2(t) = \frac{2t}{\alpha(1-\alpha)\tilde{E}} + r_0^2,$$

- $r_0 \sim 1/p_T$ - the initial dipole separation
- $\tilde{E} = p_T$ - is the dipole energy in the c.m. of the collision

FSI: attenuation of a dipole

$r_T(t)$ - evolution of a $\bar{q}q$ dipole

- applying the uncertainty relation $k_T(t) \sim 1/r_T$, we get,

$$r_T^2(t) = \frac{2t}{\alpha(1-\alpha)\tilde{E}} + r_0^2,$$

- $r_0 \sim 1/p_T$ - the initial dipole separation
- $\tilde{E} = p_T$ - is the dipole energy in the c.m. of the collision
- such a behavior of the mean separation can be also obtained within the more rigorous path integral technique for the early stage of expansion, while $r_T < r_h$ [B.Z. Kopeliovich, B.G. Zakharov; Phys. Rev. D44, 3466 (1991), B.Z. Kopeliovich, A. Schäfer, A.V. Tarasov; Phys. Rev. D62, 054022 (2000), J. Nemchik; Phys. Rev. C68, 035206 (2003)]

FSI: attenuation of a dipole

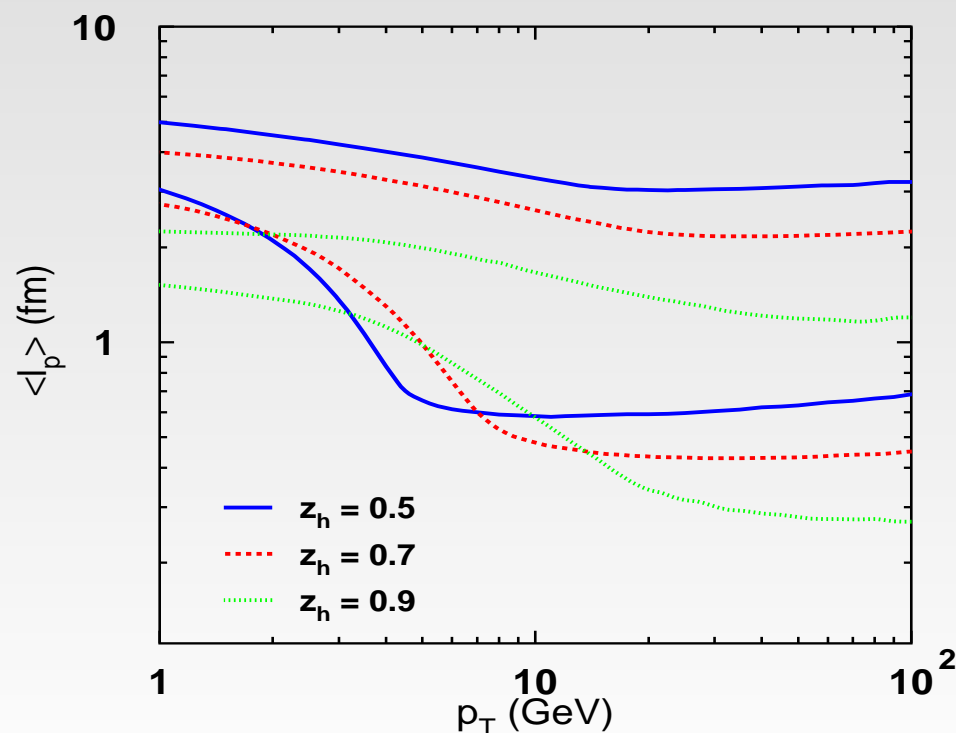
Production length of a $\bar{q}q$ dipole

- we rely on the model [B.Z. Kopeliovich, et al.; Phys. Lett. B662, 117 (2008)] for l_p - distribution of leading hadrons in a jet produced at the mid rapidity, where the initial parton energy and virtuality are equal: $E = Q = k_T = p_T/z_h = \tilde{E}/z_h$

FSI: attenuation of a dipole

Production length of a $\bar{q}q$ dipole

- we rely on the model [B.Z. Kopeliovich, et al.; Phys. Lett. B662, 117 (2008)] for l_p - distribution of leading hadrons in a jet produced at the mid rapidity, where the initial parton energy and virtuality are equal: $E = Q = k_T = p_T/z_h = \tilde{E}/z_h$
- evaluation of $\langle l_p \rangle$ in vacuum - for the quark and gluon jet



FSI: attenuation of a dipole

Survival probability

- survival probability characterizing a propagation of a dipole over path length L in a medium reads:

$$S(L) = \exp \left[- \int_0^L dl \sigma[r_T(l)] \rho_A(l) \right]$$

(dipole cross section $\sigma(r_T)$ **times** the medium density ρ_A) \equiv the **attenuation rate** of the dipole

FSI: attenuation of a dipole

Survival probability

- survival probability characterizing a propagation of a dipole over path length L in a medium reads:

$$S(L) = \exp \left[- \int_0^L dl \sigma[r_T(l)] \rho_A(l) \right]$$

(dipole cross section $\sigma(r_T)$ **times** the medium density ρ_A) \equiv the **attenuation rate** of the dipole

- the dipole cross section for small dipoles: $\sigma(r_T) = C r_T^2$, where the factor C for dipole-proton interaction is fixed from DIS data

FSI: attenuation of a dipole

Survival probability

- survival probability characterizing a propagation of a dipole over path length L in a medium reads:

$$S(L) = \exp \left[- \int_0^L dl \sigma[r_T(l)] \rho_A(l) \right]$$

(dipole cross section $\sigma(r_T)$ **times** the medium density ρ_A) \equiv the **attenuation rate** of the dipole

- the dipole cross section for small dipoles: $\sigma(r_T) = C r_T^2$, where the factor C for dipole-proton interaction is fixed from DIS data
- the factor C is unknown for a hot medium \Rightarrow it is convenient to express it in terms of the transport coefficient

FSI: attenuation of a dipole

Survival probability

- the factor C is related to the transport coefficient \hat{q} , which is broadening per unit of length:

$$C = \frac{\hat{q}}{2\rho_A}$$

[R. Baier, Yu. Dokshitzer, S. Peigne, D. Schiff; Phys. Lett. B345, 277 (1995)]

FSI: attenuation of a dipole

Survival probability

- the factor C is related to the transport coefficient \hat{q} , which is broadening per unit of length:

$$C = \frac{\hat{q}}{2\rho_A}$$

[R. Baier, Yu. Dokshitzer, S. Peigne, D. Schiff; Phys. Lett. B345, 277 (1995)]

- it was demonstrated that the same factor C controls both **dipole cross section and broadening**

[M.B. Johnson, B.Z. Kopeliovich, A.V. Tarasov; Phys. Rev. C63, 035203 (2001)]

FSI: attenuation of a dipole

Survival probability

- the factor C is related to the transport coefficient \hat{q} , which is broadening per unit of length:

$$C = \frac{\hat{q}}{2\rho_A}$$

[R. Baier, Yu. Dokshitzer, S. Peigne, D. Schiff; Phys. Lett. B345, 277 (1995)]

- it was demonstrated that the same factor C controls both **dipole cross section and broadening**

[M.B. Johnson, B.Z. Kopeliovich, A.V. Tarasov; Phys. Rev. C63, 035203 (2001)]

- then the survival probability of the dipole in a medium reads:

$$S(L) = \exp \left[-\frac{1}{2} \int_0^L dl \hat{q}(l) r_T^2(l) \right]$$

FSI: attenuation of a dipole

Survival probability

- using above mentioned expression for r_T

$$r_T^2(l) = \frac{2l}{\alpha(1-\alpha)\tilde{E}} + r_0^2$$

FSI: attenuation of a dipole

Survival probability

- using above mentioned expression for r_T

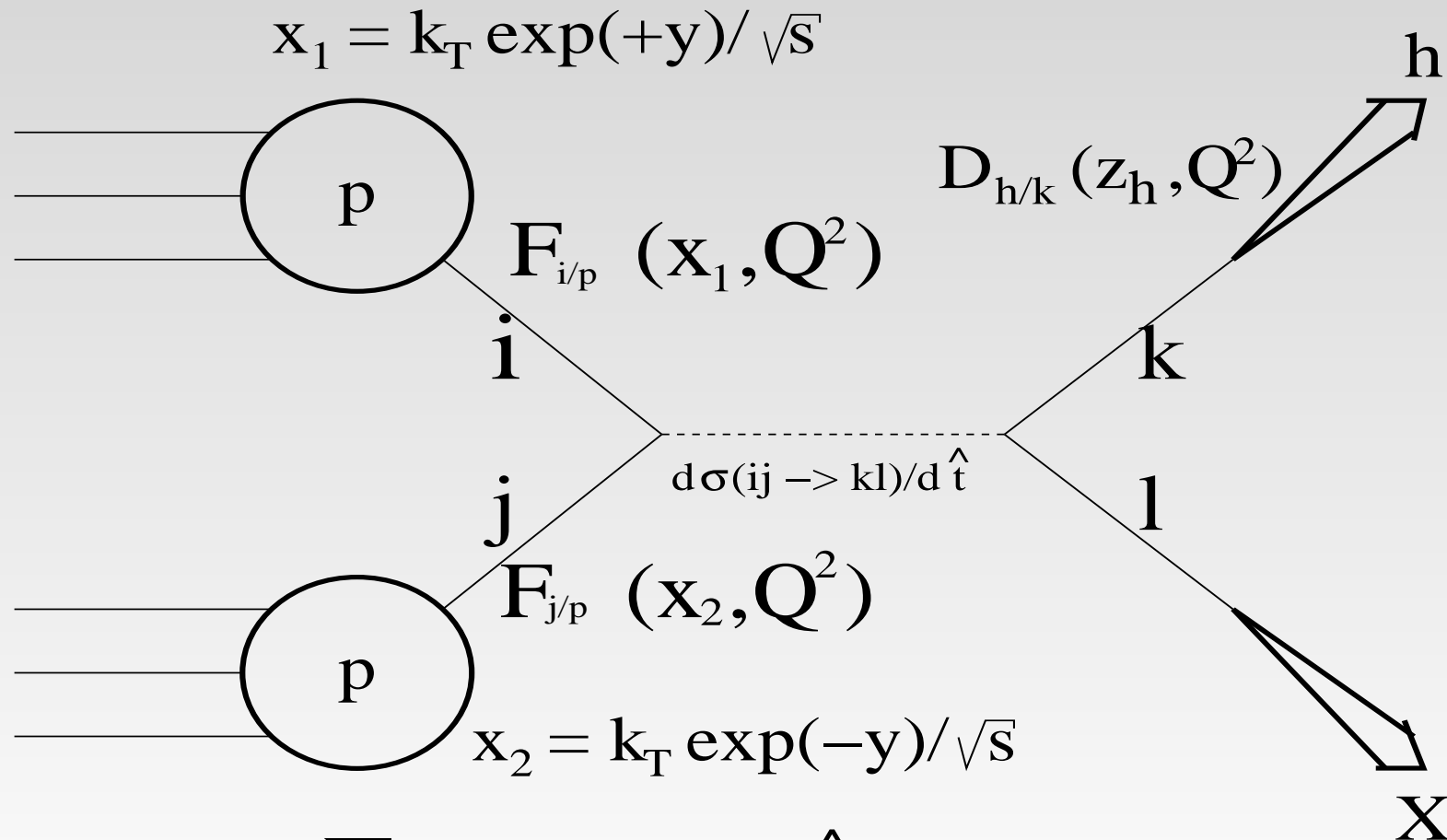
$$r_T^2(l) = \frac{2l}{\alpha(1-\alpha)} \tilde{E} + r_0^2$$

- and neglecting $r_0^2 \sim 1/p_T^2$ at large p_T , we get the final expression for the survival probability of the dipole in a medium

$$S(L) = \exp \left[-\frac{1}{\alpha(1-\alpha)p_T} \int_0^L dl \hat{q}(l) l \right]$$

High- p_T hadrons in $p + p$ collisions

cross section of the reaction, $p + p \rightarrow h + X$, is calculated using standard convolution expression based on QCD factorization:



$$\sigma_{pp}(p_T) = \sum_{i,j,k,l} F_{i/p} \otimes F_{j/p} \otimes \hat{\sigma}(ij \rightarrow kl) \otimes D_{h/k}$$

High- p_T hadrons in $A + B$ collisions



- the cross section of the reaction, $A + B \rightarrow h + X$, at given impact parameter b reads

$$\sigma_{AB}(b, p_T) = \int_0^\infty d^2\tau T_A(\tau) T_B(\vec{b} - \vec{\tau}) \times$$
$$\sum_{i,j,k,l} F_{i/A} \otimes F_{j/B} \otimes \hat{\sigma}_{ij \rightarrow kl} \otimes \tilde{D}_{h/k} R_{AB}^k(\vec{b}, \vec{\tau}, p_T)$$

High- p_T hadrons in $A + B$ collisions



- the factor $R_{AB}^k(\vec{b}, \vec{\tau}, p_T)$ in expression for $\sigma_{AB}(b, p_T)$ - corresponds to a survival probability of a $\bar{q}q$ - the nuclear suppression factor in a collision of two heavy nuclei at given impact parameter \vec{b} corresponding to production of a high- k_T parton of species k at impact parameter $\vec{\tau}$, propagating then over a path length $\langle l_p \rangle$, radiating gluons and losing energy, and eventually producing a colorless dipole pre-hadron with transverse momentum $\vec{p}_T = \vec{k}_T z_h$ (z_h is a fraction of the jet momentum carried by the produced hadron), which propagates through the nucleus evolving its size according to $r_T^2(t)$

High- p_T hadrons in $A + B$ collisions



- the suppression factor $R_{AB}^k(\vec{b}, \vec{\tau}, p_T)$ has the form,

$$R_{AB}^k(\vec{b}, \vec{\tau}, p_T) = \int_0^\pi \frac{d\phi}{\pi} \exp \left[-\frac{1}{\alpha(1-\alpha)p_T} \int_{l_{max}^k(p_T, z_h)}^\infty dl l \hat{q}(l, \vec{b}, \vec{\tau} + \vec{l}) \right]$$

High- p_T hadrons in $A + B$ collisions



- the suppression factor $R_{AB}^k(\vec{b}, \vec{\tau}, p_T)$ has the form,

$$R_{AB}^k(\vec{b}, \vec{\tau}, p_T) = \int_0^\pi \frac{d\phi}{\pi} \exp \left[-\frac{1}{\alpha (1 - \alpha) p_T} \int_{l_{max}^k(p_T, z_h)}^\infty dl l \hat{q}(l, \vec{b}, \vec{\tau} + \vec{l}) \right]$$

- $l_{max}^k(p_T, z_h) = \max\{\langle l_p^k(p_T, z_h) \rangle, l_0\}$ and
 $t_0 = l_0 \sim 1$ fm is the time scale of creation of the medium
resulted from gluon radiation at mid rapidities in HIC

High- p_T hadrons in $A + B$ collisions



- the suppression factor $R_{AB}^k(\vec{b}, \vec{\tau}, p_T)$ has the form,

$$R_{AB}^k(\vec{b}, \vec{\tau}, p_T) = \int_0^\pi \frac{d\phi}{\pi} \exp \left[-\frac{1}{\alpha (1 - \alpha) p_T} \int_{l_{max}^k(p_T, z_h)}^\infty dl l \hat{q}(l, \vec{b}, \vec{\tau} + \vec{l}) \right]$$

- $l_{max}^k(p_T, z_h) = \max\{\langle l_p^k(p_T, z_h) \rangle, l_0\}$ and
 $t_0 = l_0 \sim 1$ fm is the time scale of creation of the medium resulted from gluon radiation at mid rapidities in HIC
- the production length for a gluon jet ($k = g$) is short,
 $\langle l_p^g \rangle \lesssim l_0 \Rightarrow$ its actual value is not important at LHC

High- p_T hadrons in $A + B$ collisions



- the suppression factor $R_{AB}^k(\vec{b}, \vec{\tau}, p_T)$ has the form,

$$R_{AB}^k(\vec{b}, \vec{\tau}, p_T) = \int_0^\pi \frac{d\phi}{\pi} \exp \left[- \frac{1}{\alpha (1 - \alpha) p_T} \int_{l_{max}^k(p_T, z_h)}^\infty dl l \hat{q}(l, \vec{b}, \vec{\tau} + \vec{l}) \right]$$

- $l_{max}^k(p_T, z_h) = \max\{\langle l_p^k(p_T, z_h) \rangle, l_0\}$ and $t_0 = l_0 \sim 1$ fm is the time scale of creation of the medium resulted from gluon radiation at mid rapidities in HIC
- the production length for a gluon jet ($k = g$) is short, $\langle l_p^g \rangle \lesssim l_0 \Rightarrow$ its actual value is not important at LHC
- a dominance of quarks at RHIC energies corresponds to much higher $\langle l_p^q \rangle > l_0$ in a broad range of p_T - and z_h -values \Rightarrow this causes a weaker nuclear suppression in comparison with the LHC kinematic region

High- p_T hadrons in $A + B$ collisions



- although above evaluation of $\langle l_p^k \rangle$ in vacuum gives a dominant contribution to nuclear suppression we include also the medium-induced E-loss during propagation of a parton species k corresponding to mean production length, $\langle l_p^k \rangle$.

High- p_T hadrons in $A + B$ collisions



- although above evaluation of $\langle l_p^k \rangle$ in vacuum gives a dominant contribution to nuclear suppression we include also the medium-induced E-loss during propagation of a parton species k corresponding to mean production length, $\langle l_p^k \rangle$.
- this was realized via modification of the fragmentation function $D_{h/k} \Rightarrow \hat{D}_{h/k}$ shifting z_h to $\tilde{z}_h = z_h E / (E - \Delta E_{in})$

High- p_T hadrons in $A + B$ collisions



- although above evaluation of $\langle l_p^k \rangle$ in vacuum gives a dominant contribution to nuclear suppression we include also the medium-induced E-loss during propagation of a parton species k corresponding to mean production length, $\langle l_p^k \rangle$.
- this was realized via modification of the fragmentation function $D_{h/k} \Rightarrow \hat{D}_{h/k}$ shifting z_h to $\tilde{z}_h = z_h E / (E - \Delta E_{in})$
- the medium-induced energy loss $\Delta E_{in} = \kappa_{in} (l_p^k - l_0) \Theta(l_p^k - l_0)$, where $\Theta(l)$ represents the step function and the rate of energy loss κ_{in} was evaluated in [R. Baier, Yu. Dokshitzer, A. Mueller, S. Peigne, D. Schiff; Nucl. Phys. B484, 265 (1997)]

High- p_T hadrons in $A + B$ collisions



- the rate κ_{in} corresponding to $\langle l_p^k \rangle$ reads,

$$\kappa_{in} = \frac{\alpha_S N_C}{8} \hat{q}(l_p^k, \vec{b}, \vec{\tau}) l_p^k$$

High- p_T hadrons in $A + B$ collisions



- the rate κ_{in} corresponding to $\langle l_p^k \rangle$ reads,

$$\kappa_{in} = \frac{\alpha_S N_C}{8} \hat{q}(l_p^k, \vec{b}, \vec{\tau}) l_p^k$$

- in the LHC kinematic region an inclusion of the medium-induced E-loss is irrelevant due to a dominance of gluon jets ($k = g$) and consequent shortness of the mean $\langle l_p^g \rangle \lesssim l_0$

Green function approach

- the corresponding suppression factor

$$R_{AB}^k(\vec{b}, \vec{\tau}, p_T) = \frac{\int_0^{2\pi} \frac{d\phi}{2\pi} \left| \int_0^1 d\alpha \int d^2r_1 d^2r_2 \Psi_h^\dagger(\vec{r}_2, \alpha) G_{\bar{q}q}(\vec{b}, \vec{\tau}; l_1, \vec{r}_1; l_2, \vec{r}_2) \Psi_{in}(\vec{r}_1, \alpha) \right|^2}{\left| \int_0^1 d\alpha \int d^2r_1 d^2r_2 \Psi_h^\dagger(\vec{r}_2, \alpha) \Psi_{in}(\vec{r}_1, \alpha) \right|^2}$$

[B.Z. Kopeliovich, J.N., I.K. Potashnikova, I. Schmidt, Phys. Rev. C86, 054904 (2012)]

Green function approach

- the corresponding suppression factor

$$R_{AB}^k(\vec{b}, \vec{\tau}, p_T) = \frac{\int_0^{2\pi} \frac{d\phi}{2\pi} \left| \int_0^1 d\alpha \int d^2r_1 d^2r_2 \Psi_h^\dagger(\vec{r}_2, \alpha) G_{\bar{q}q}(\vec{b}, \vec{\tau}; l_1, \vec{r}_1; l_2, \vec{r}_2) \Psi_{in}(\vec{r}_1, \alpha) \right|^2}{\left| \int_0^1 d\alpha \int d^2r_1 d^2r_2 \Psi_h^\dagger(\vec{r}_2, \alpha) \Psi_{in}(\vec{r}_1, \alpha) \right|^2}$$

- where the Green function satisfies the two-dimensional Schroedinger equation:

$$\left[i \frac{d}{dl_2} - \frac{m_q^2 - \Delta_{r_2}}{2 p_T \alpha (1 - \alpha)} - V_{\bar{q}q}(\vec{b}, \vec{\tau}; l_2, \vec{r}_2) \right] G_{\bar{q}q}(\vec{b}, \vec{\tau}; l_1, \vec{r}_1; l_2, \vec{r}_2) = i\delta(l_2 - l_1) \delta(\vec{r}_2 - \vec{r}_1),$$

[B.Z. Kopeliovich, J.N., I.K. Potashnikova, I. Schmidt, Phys. Rev. C86, 054904 (2012)]

Green function approach

- with the boundary conditions

$$G_{\bar{q}q}(l_1, \vec{r}_1; l_2, \vec{r}_2) \Big|_{l_1=l_2} = \delta(\vec{r}_2 - \vec{r}_1);$$
$$G_{\bar{q}q}(l_1, \vec{r}_1; l_2, \vec{r}_2) \Big|_{l_1>l_2} = 0$$

Green function approach

- with the boundary conditions

$$G_{\bar{q}q}(l_1, \vec{r}_1; l_2, \vec{r}_2) \Big|_{l_1=l_2} = \delta(\vec{r}_2 - \vec{r}_1);$$

$$G_{\bar{q}q}(l_1, \vec{r}_1; l_2, \vec{r}_2) \Big|_{l_1>l_2} = 0$$

- The imaginary part of the light-cone potential $V_{\bar{q}q}(\vec{b}, \vec{\tau}; l_2, \vec{r}_2)$ is responsible for absorption in the medium:

$$\text{Im} V_{\bar{q}q}(\vec{b}, \vec{\tau}; l, \vec{r}) = -\frac{1}{4} \hat{q}(l, \vec{b}, \vec{\tau}) r^2.$$

What are the observables ?

- nuclear attenuation (modification) factor at given impact parameter b

$$R_{AB}(b, p_T) = \frac{\sigma_{AB}(b, p_T)}{\int_0^{\infty} d^2\tau T_A(\tau) T_B(\vec{b} - \vec{\tau}) \sigma_{pp}(p_T)}$$

What are the observables ?

- nuclear attenuation (modification) factor at given impact parameter b

$$R_{AB}(b, p_T) = \frac{\sigma_{AB}(b, p_T)}{\int_0^\infty d^2\tau T_A(\tau) T_B(\vec{b} - \vec{\tau}) \sigma_{pp}(p_T)}$$

- observable sensitive to the properties of the created medium
 - azimuthal asymmetry of the produced hadrons relative to the reaction plane \Rightarrow it is characterized by the parameter - **elliptic flow** at given impact parameter b

$$v_2(b, p_T) = \langle \cos(2\phi) \rangle = \frac{\hat{\sigma}_{AB}(b, p_T)}{\sigma_{AB}(b, p_T)},$$

What are the observables ?

where

$$\hat{\sigma}_{AB}(b, p_T) = \int_0^\infty d^2\tau T_A(\tau) T_B(\vec{b} - \vec{\tau}) \times$$

$$\sum_{i,j,k,l} F_{i/A}^{(B)}(\vec{\tau}) \otimes F_{j/B}^{(A)}(\vec{b} - \vec{\tau}) \otimes \hat{\sigma}_{ij \rightarrow kl} \otimes \tilde{D}_{h/k} \hat{R}_{AB}^k(\vec{b}, \vec{\tau}, p_T),$$

What are the observables ?

where

$$\hat{\sigma}_{AB}(b, p_T) = \int_0^\infty d^2\tau T_A(\tau) T_B(\vec{b} - \vec{\tau}) \times$$

$$\sum_{i,j,k,l} F_{i/A}^{(B)}(\vec{\tau}) \otimes F_{j/B}^{(A)}(\vec{b} - \vec{\tau}) \otimes \hat{\sigma}_{ij \rightarrow kl} \otimes \tilde{D}_{h/k} \hat{R}_{AB}^k(\vec{b}, \vec{\tau}, p_T),$$

and the modified suppression factor - simple model

$$\hat{R}_{AB}^k(\vec{b}, \vec{\tau}, p_T) = \int_0^\pi \frac{d\phi}{\pi} \cos(2\phi) \times$$

$$\exp \left[-\frac{1}{\alpha (1 - \alpha) p_T} \int_{l_{max}^k(p_T, z_h)}^\infty dl l \hat{q}(l, \vec{b}, \vec{\tau} + \vec{l}) \right].$$

What are the observables ?

- and the modified suppression factor - Green function formalism

$$\hat{R}_{AB}^k(\vec{b}, \vec{\tau}, p_T) =$$

$$\frac{\int_0^{2\pi} \frac{d\phi}{2\pi} \cos(2\phi) \left| \int_0^1 d\alpha \int d^2r_1 d^2r_2 \Psi_h^\dagger(\vec{r}_2, \alpha) G_{\bar{q}q}(\vec{b}, \vec{\tau}; l_1, \vec{r}_1; l_2, \vec{r}_2) \Psi_{in}(\vec{r}_1, \alpha) \right|^2}{\left| \int_0^1 d\alpha \int d^2r_1 d^2r_2 \Psi_h^\dagger(\vec{r}_2, \alpha) \Psi_{in}(\vec{r}_1, \alpha) \right|^2}$$

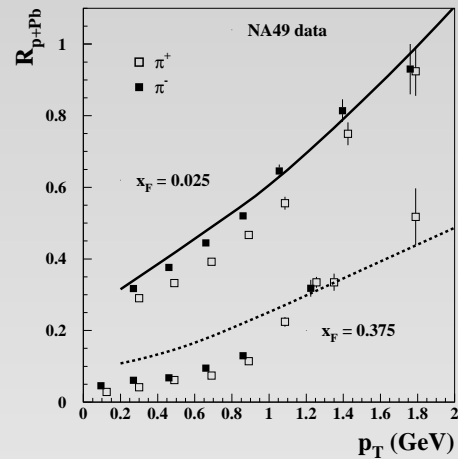
ISI: energy conservation constraints



Any reaction observed so far at any energy is nuclear suppressed at forward rapidities.

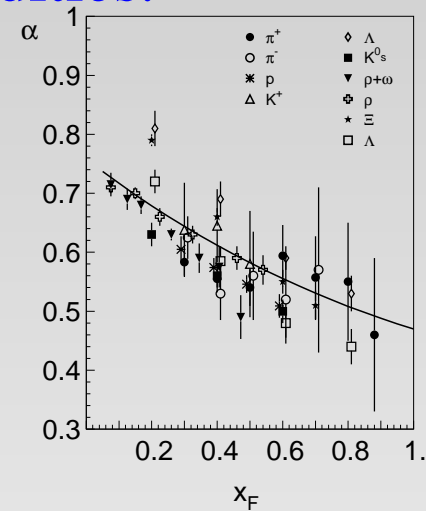
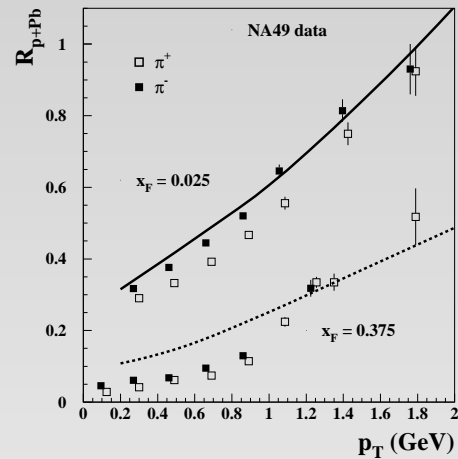
ISI: energy conservation constraints

Any reaction observed so far at any energy is nuclear suppressed at forward rapidities.



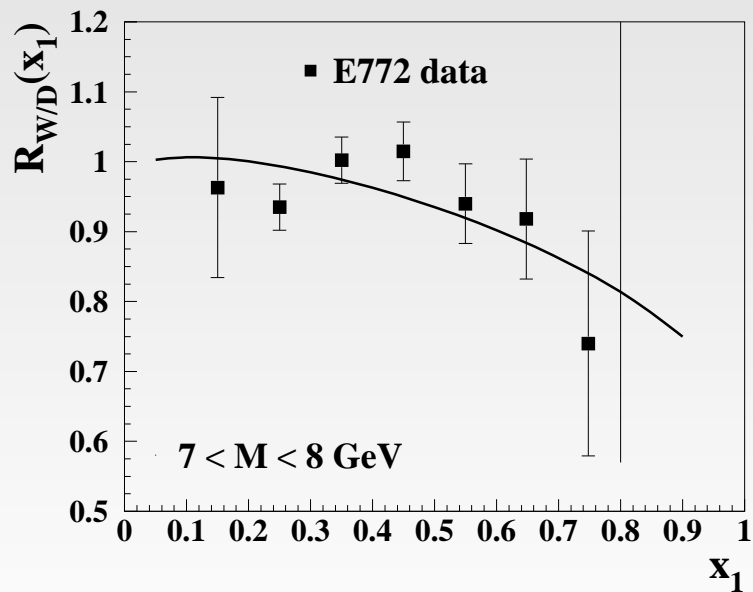
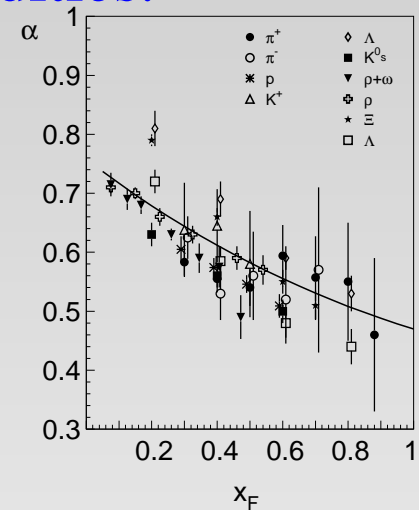
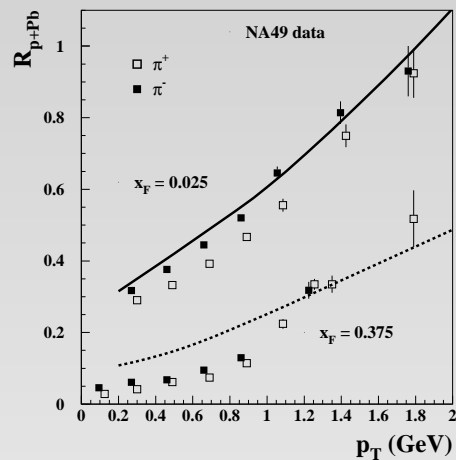
ISI: energy conservation constraints

Any reaction observed so far at any energy is nuclear suppressed at forward rapidities.



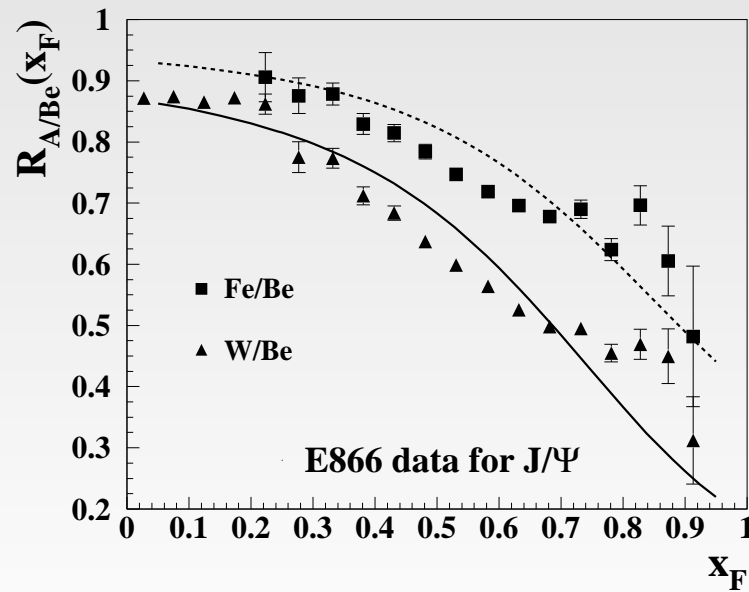
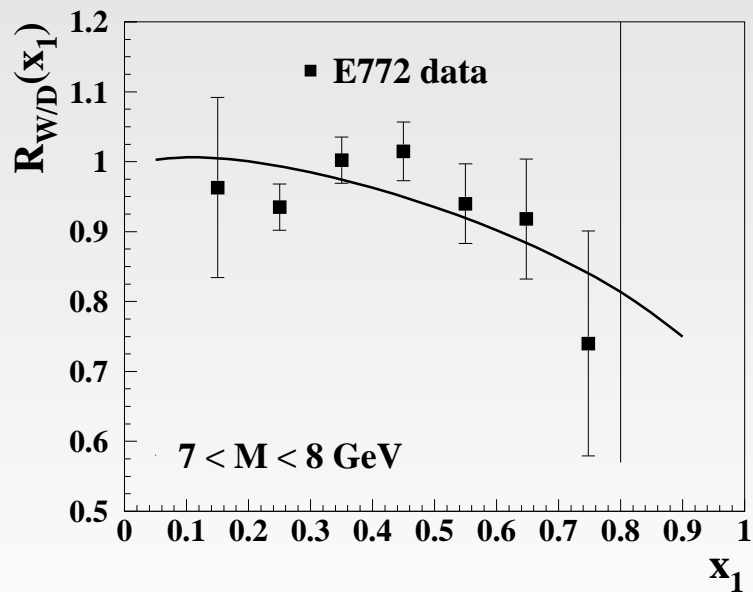
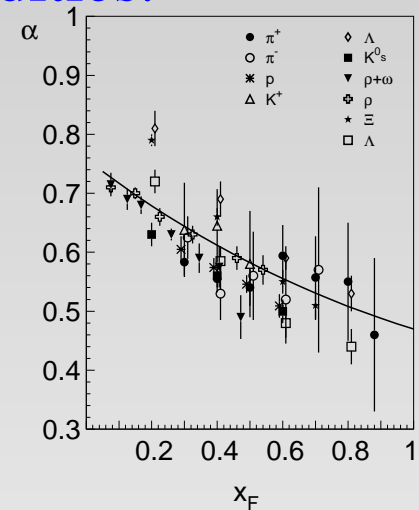
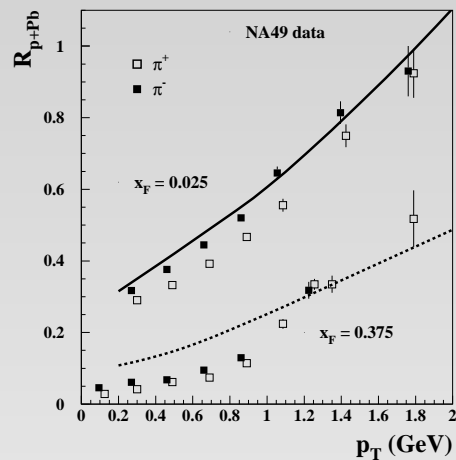
ISI: energy conservation constraints

Any reaction observed so far at any energy is nuclear suppressed at forward rapidities.



ISI: energy conservation constraints

Any reaction observed so far at any energy is nuclear suppressed at forward rapidities.



ISI: energy conservation constraints



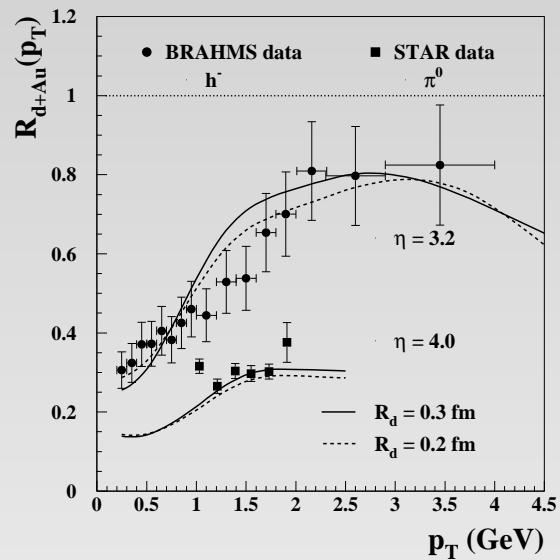
One can approach the kinematic limit increasing either x_F , or

$$x_T = 2p_T / \sqrt{s}.$$

ISI: energy conservation constraints

One can approach the kinematic limit increasing either x_F , or

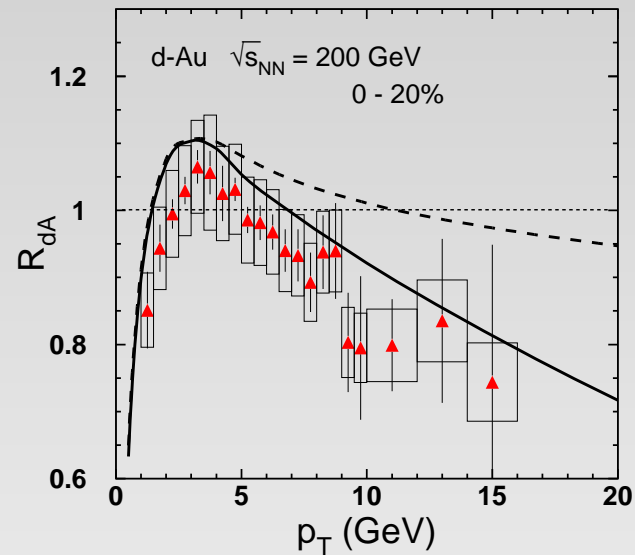
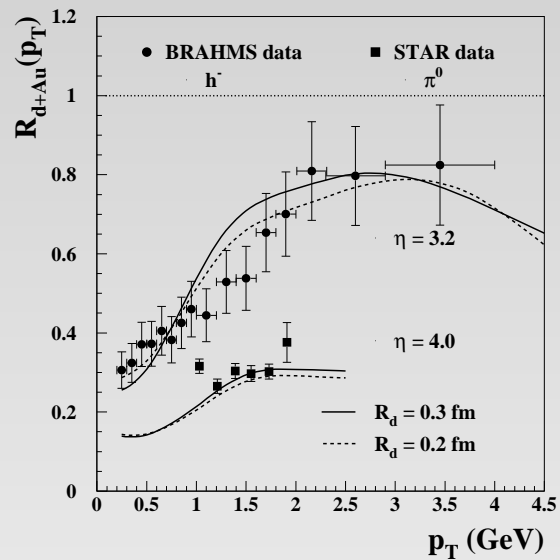
$$x_T = 2p_T / \sqrt{s}.$$



ISI: energy conservation constraints

One can approach the kinematic limit increasing either x_F , or

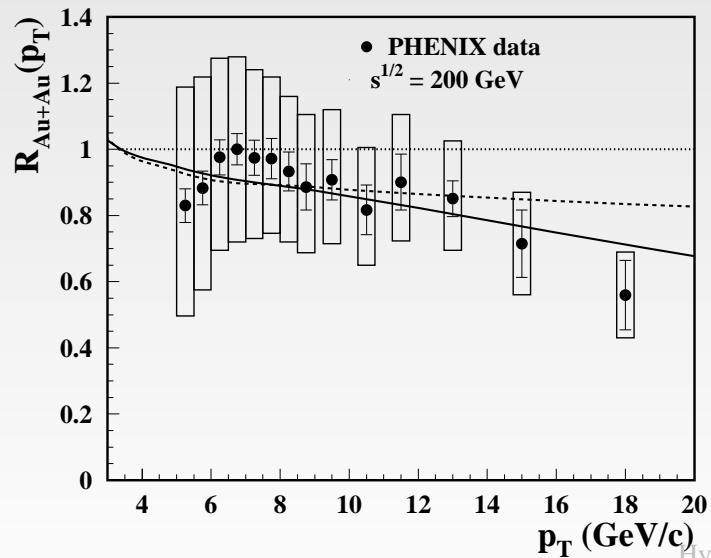
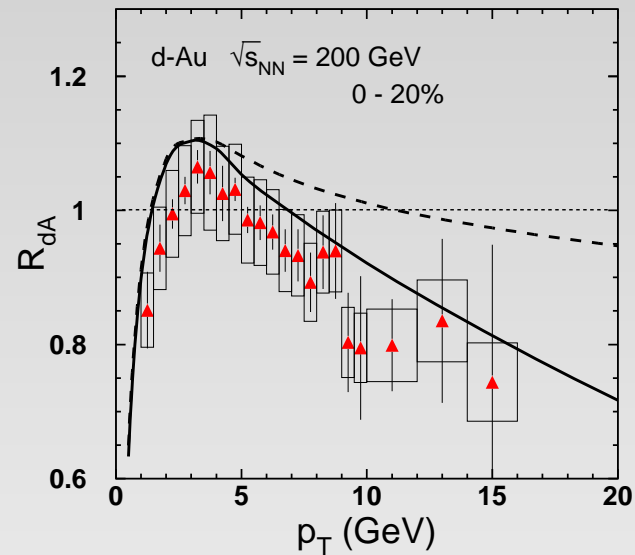
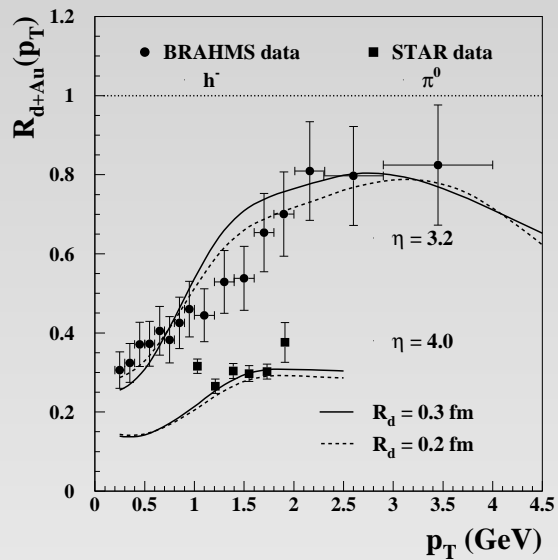
$$x_T = 2p_T / \sqrt{s}.$$



ISI: energy conservation constraints

One can approach the kinematic limit increasing either x_F , or

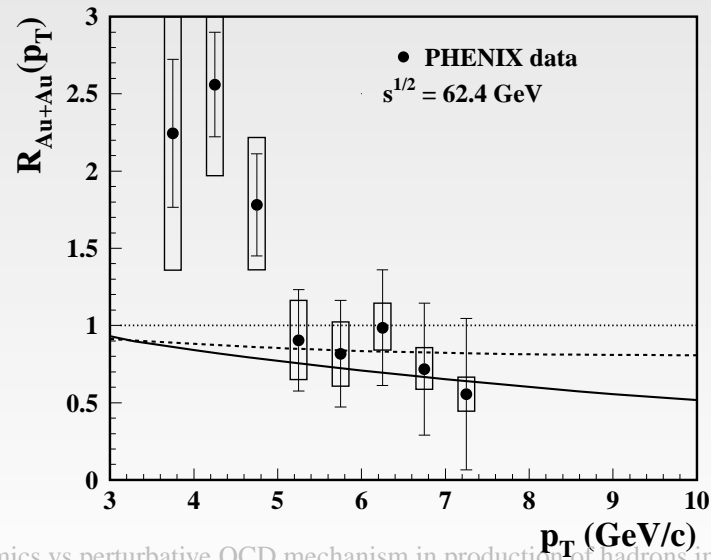
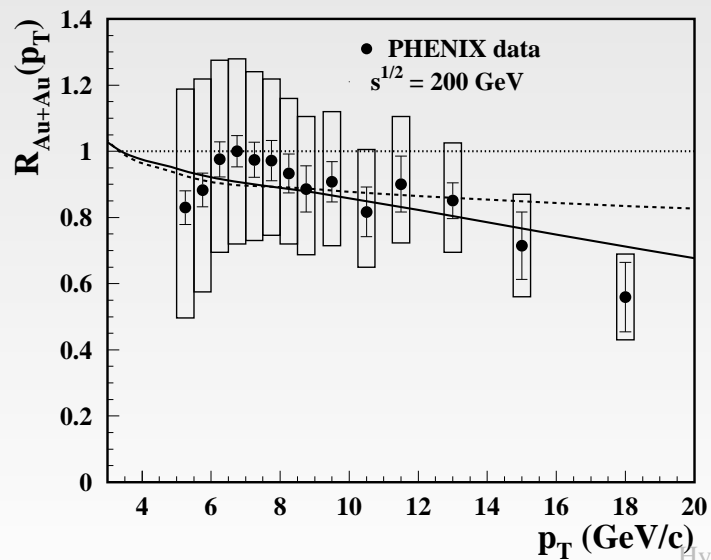
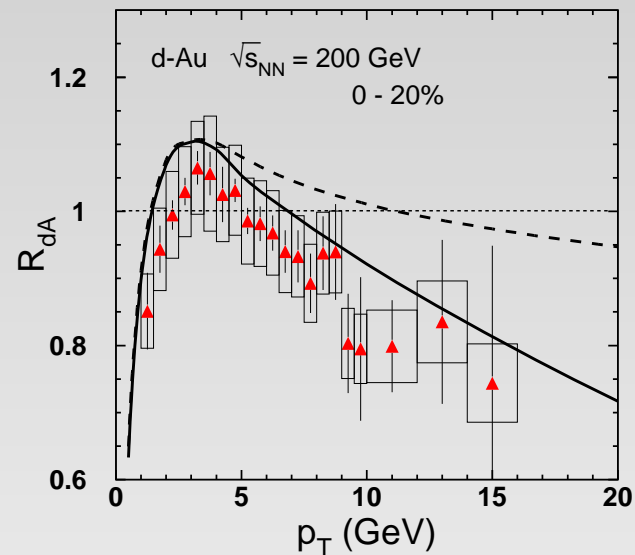
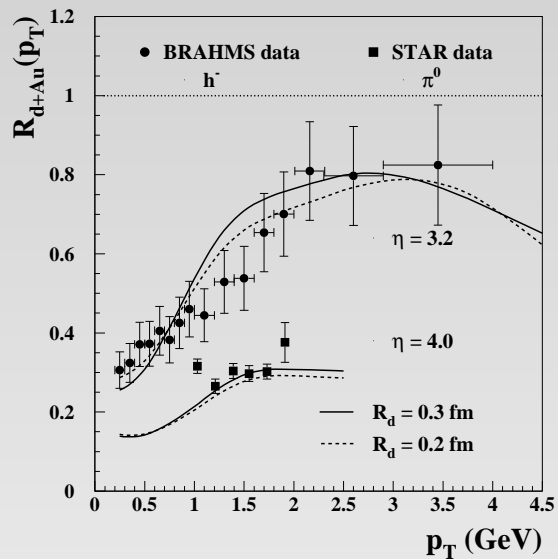
$$x_T = 2p_T / \sqrt{s}.$$



ISI: energy conservation constraints

One can approach the kinematic limit increasing either x_F , or

$$x_T = 2p_T / \sqrt{s}.$$



Interpretations of ISI suppression

Since the kinematic limit can be approached increasing either x_F or p_T , it is convenient to introduce a variable ξ ,

$$\xi = \sqrt{x_F^2 + x_T^2},$$

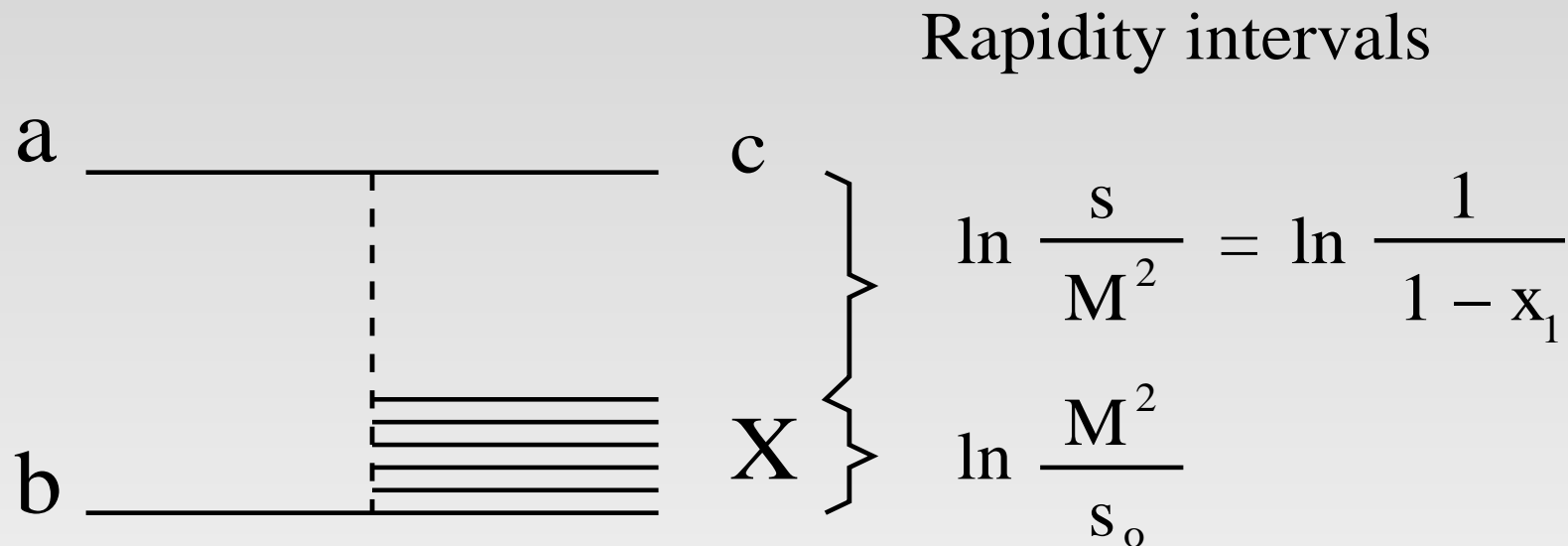
where

$$x_F = \frac{2 p_L}{\sqrt{s}}, \quad x_T = \frac{2 p_T}{\sqrt{s}}.$$

Here p_L and p_T is the longitudinal and transverse component of the momentum of the produced particles in c.m. frame.

Interpretations of ISI suppression

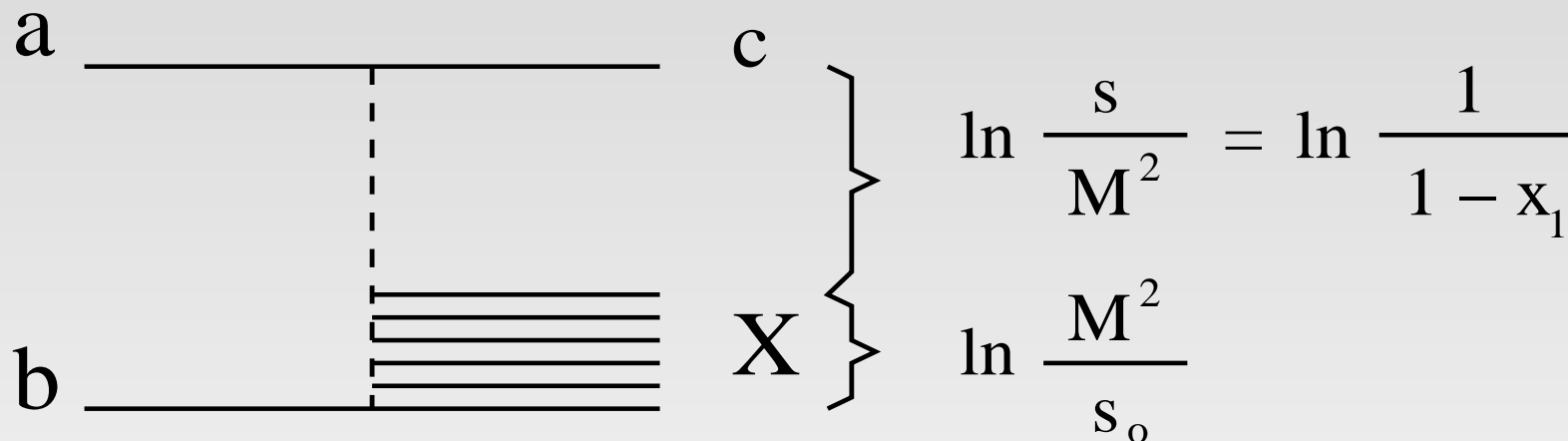
- any reaction, $a + b \rightarrow c + X$, where $c = h, \bar{l}l, J/\Psi, \dots$ is a large rapidity gap (LRG) process at $\xi \rightarrow 1$



Interpretations of ISI suppression

- any reaction, $a + b \rightarrow c + X$, where $c = h, \bar{l}l, J/\Psi, \dots$ is a large rapidity gap (LRG) process at $\xi \rightarrow 1$

Rapidity intervals



- the probability to radiate no gluons in the rapidity interval $\Delta y = \ln \frac{1}{1-\xi}$ is suppressed by the **SUDAKOV'S FORM FACTOR** $S(\Delta y) = 1 - \xi$, which violates QCD factorization

Interpretations of ISI suppression

- assuming $A + B$ collisions and summing over multiple interactions, the parton distribution in N of the projectile nucleus A can be expressed in terms of $T_B(b)$ and the effective $\sigma_{eff} \sim \sigma_{in}^{hN} = 20 \text{ mb}$

[B.Z. Kopeliovich, J. Nemchik, I.K. Potashnikova, M.B. Johnson, I. Schmidt; PR C72, 054606 (2005)]

$$F_{i/N}^{(B)}(x_1, k_{1,T}^2, b) = C_G F_{i/N}(x_1, k_{1,T}^2) \frac{e^{-[1-S(\xi)]\sigma_{eff}T_B(b)} - e^{-\sigma_{eff}T_B(b)}}{S(\xi) [1 - e^{-\sigma_{eff}T_B(b)}]}$$

the normalization factor C_G is fixed by the Gottfried sum rule

Interpretations of ISI suppression

- assuming $A + B$ collisions and summing over multiple interactions, the parton distribution in N of the projectile nucleus A can be expressed in terms of $T_B(b)$ and the effective $\sigma_{eff} \sim \sigma_{in}^{hN} = 20 mb$

[B.Z. Kopeliovich, J. Nemchik, I.K. Potashnikova, M.B. Johnson, I. Schmidt; PR C72, 054606 (2005)]

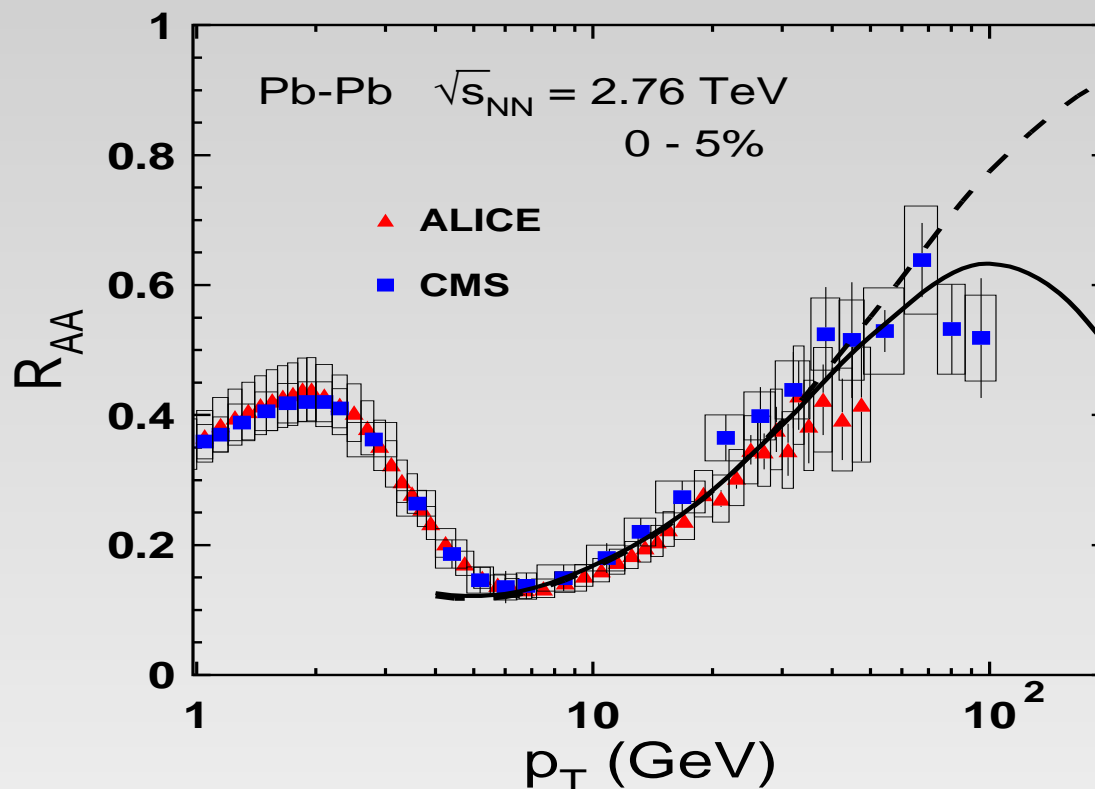
$$F_{i/N}^{(B)}(x_1, k_{1,T}^2, b) = C_G F_{i/N}(x_1, k_{1,T}^2) \frac{e^{-[1-S(\xi)]\sigma_{eff}T_B(b)} - e^{-\sigma_{eff}T_B(b)}}{S(\xi) [1 - e^{-\sigma_{eff}T_B(b)}]}$$

the normalization factor C_G is fixed by the Gottfried sum rule

- in $A + B$ collisions one should take into account also multiple interactions of target partons of the nucleus B in the projectile nucleus A leading to the same form of effective parton distributions $F_{j/N}^{(A)}$ except that one should replace $x_1 \Rightarrow x_2, k_{1,T} \Rightarrow k_{2,T}, B \Rightarrow A, T_B \Rightarrow T_A$

Numerical results vs. data

Comparison with LHC data



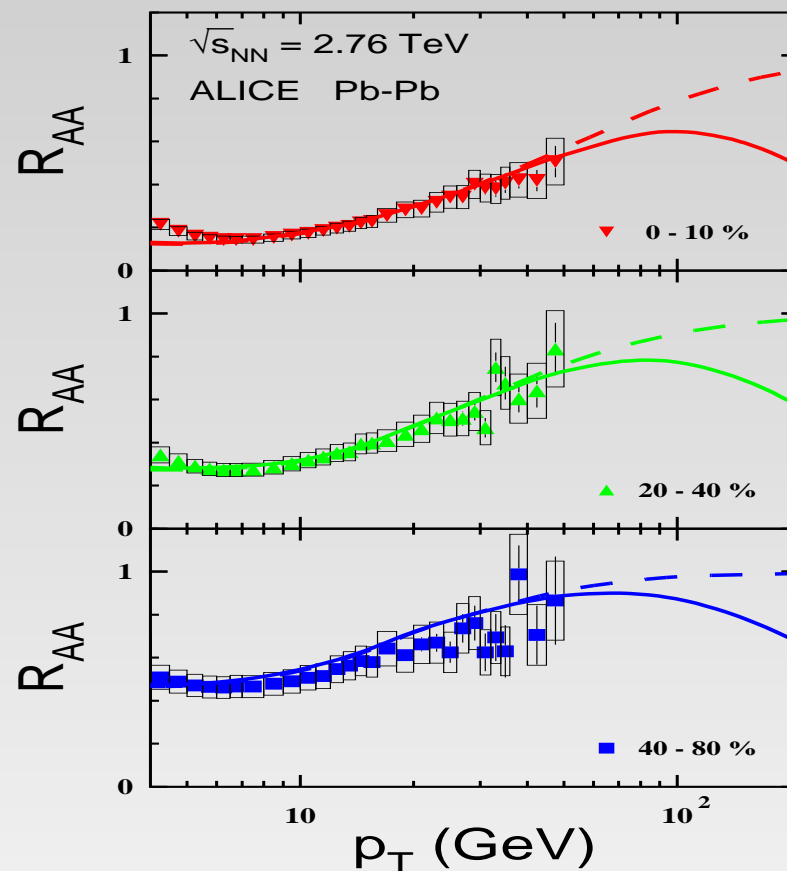
ALICE and CMS data for central, 0-5%, lead-lead collisions vs. the GF formalism at adjusted $\hat{q}_0 = 2.0 \text{ GeV}^2 / \text{fm}$.

[TRIANGLES - ALICE Collaboration, B. Abelev et al.; Phys. Lett. B720, 52 (2013).]

[SQUARES - CMS Collaboration, Y.-J. Lee et al.; J. Phys. G 38, 124015 (2011). A. S. Yoon et al.; J. Phys. G 38, 124116 (2011).]

Numerical results vs. data

Comparison with LHC data - ALICE

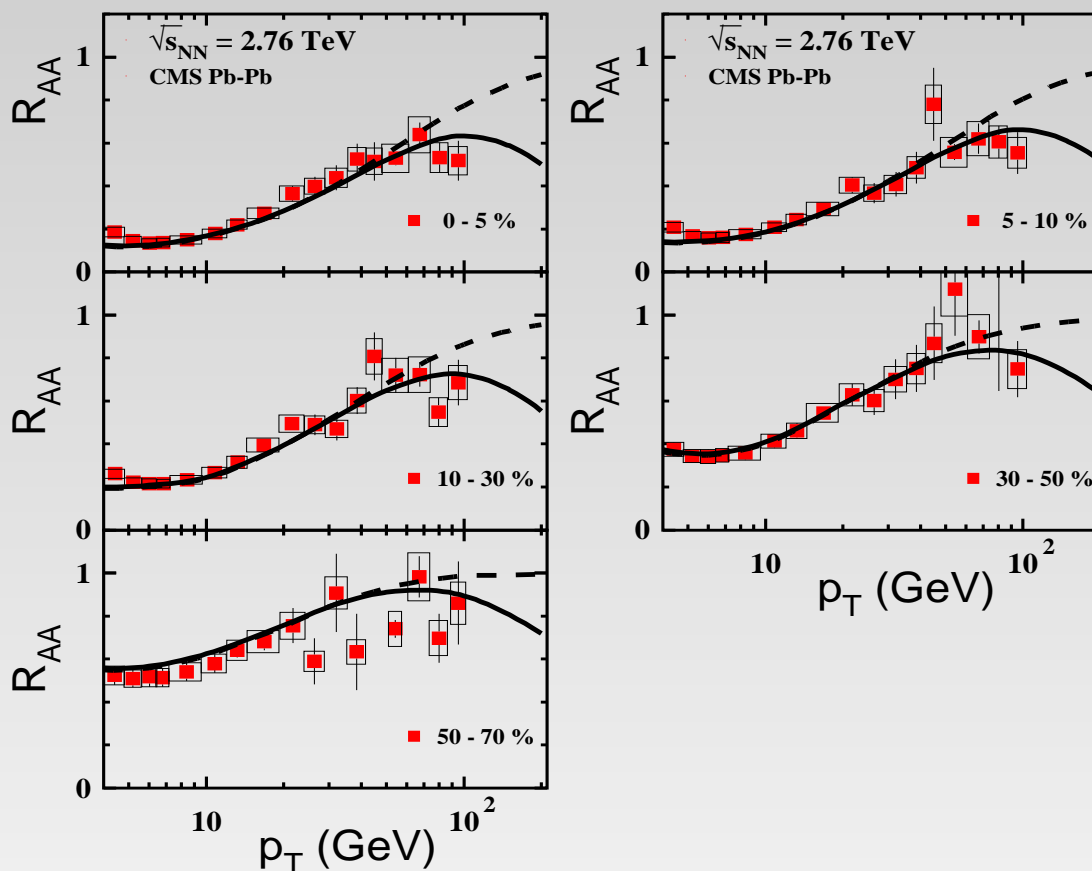


$R_{AA}(p_T)$ for charge hadrons produced in lead-lead collisions at different centralities. Calculations within the GF formalism with $\hat{q}_0 = 2.0 \text{ GeV}^2/\text{fm}$ are compared with ALICE data.

[ALICE Collaboration, B. Abelev et al.; Phys. Lett. B720, 52 (2013).]

Numerical results vs. data

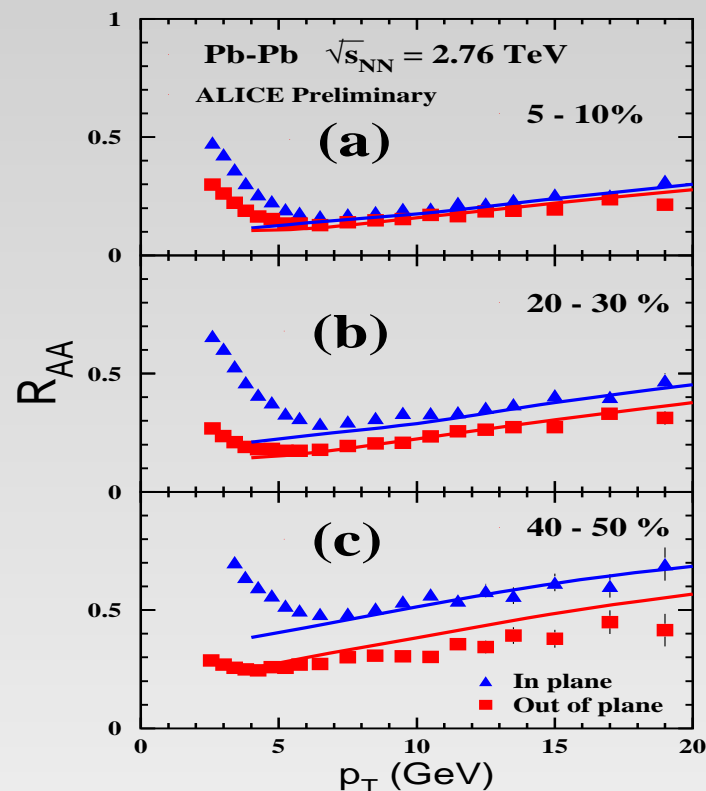
Comparison with LHC data - CMS



$R_{AA}(p_T)$ for charge hadrons produced in lead-lead collisions at different centralities. Calculations within the GF formalism with $\hat{q}_0 = 2.0$ GeV²/fm are compared with CMS data.

Numerical results vs. data

Comparison with LHC data - azimuthal asymmetry

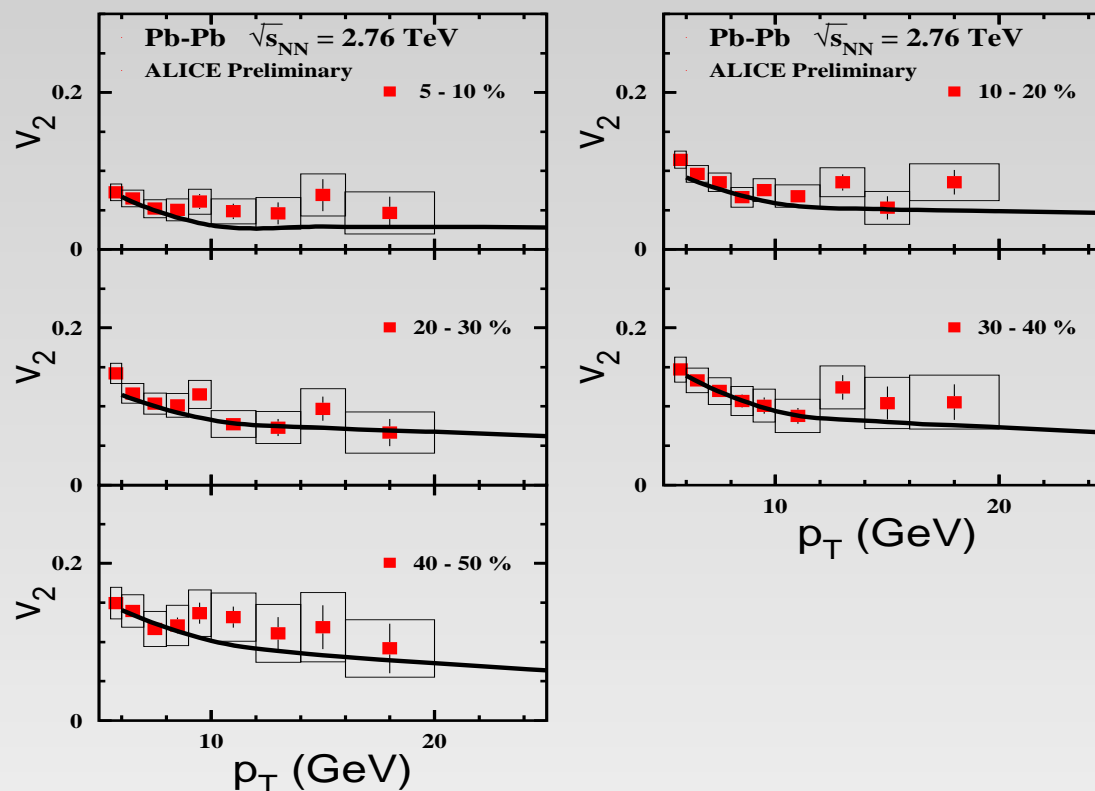


$R_{AA}(p_T)$ for charge hadrons produced in lead-lead collisions for two classes of events: In plane ($-45^\circ \leq \phi \leq 45^\circ$) and Out-of-plane ($45^\circ \leq \phi \leq 135^\circ$). The GF calculations with $\hat{q}_0 = 2.0 \text{ GeV}^2/\text{fm}$ are compared with ALICE data.

[ALICE Collaboration, A. Dobrin et al.; J. Phys. G **38**, 124170 (2011).]

Numerical results vs. data

Comparison with LHC data - azimuthal asymmetry

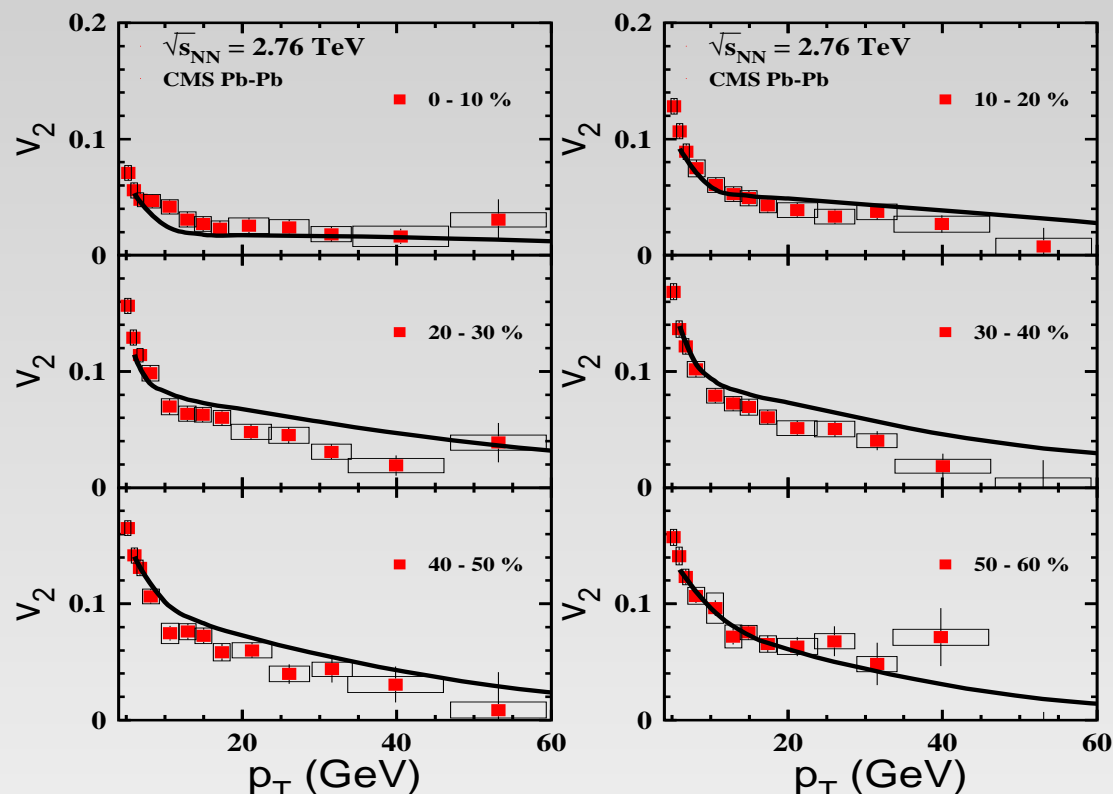


Azimuthal anisotropy $v_2(p_T)$ for charge hadron production in lead-lead collisions at different centralities 5-10%, 10-20%, 20-30%, 30-40%, 40-50%. The GF calculations with $\hat{q}_0 = 2.0 \text{ GeV}^2 / \text{fm}$ are compared with ALICE data.

[ALICE Collaboration, A. Dobrin et al.; J. Phys. G **38**, 124170 (2011).]

Numerical results vs. data

Comparison with LHC data - azimuthal asymmetry

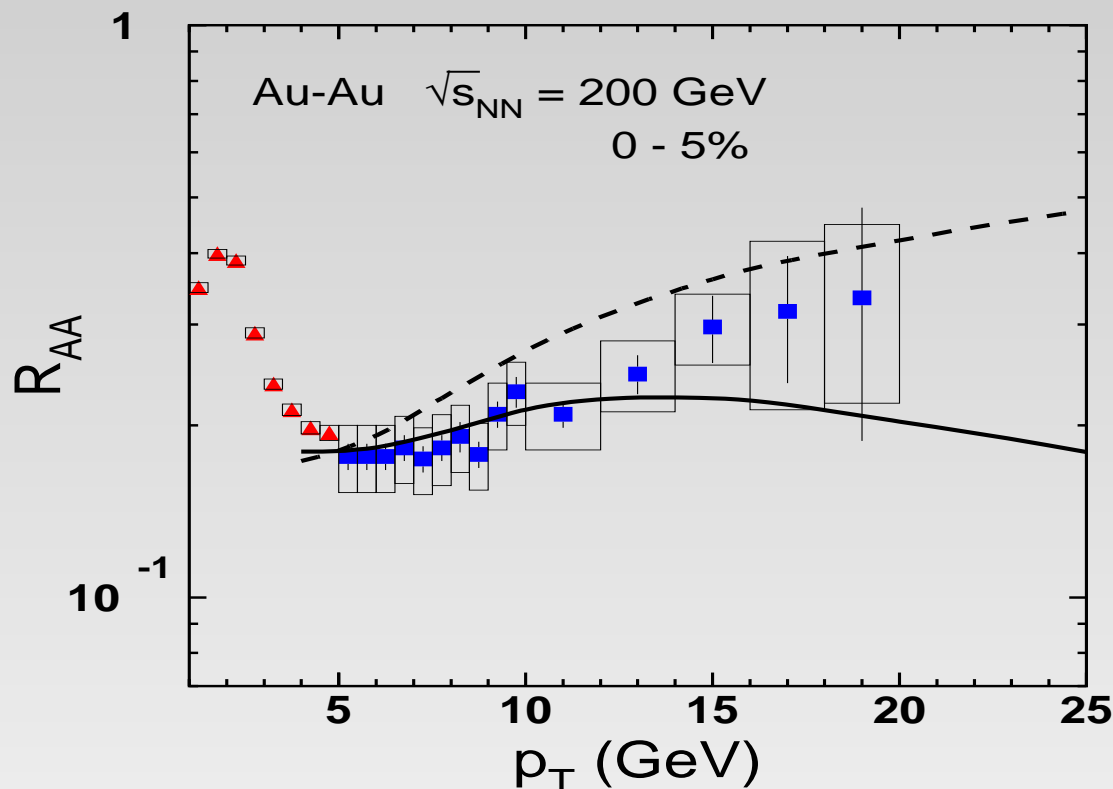


Azimuthal anisotropy $v_2(p_T)$ for charge hadron production in lead-lead collisions at different centralities 0-10%, 10-20%, 20-30%, 30-40%, 40-50%, 50-60%. The GF calculations with $\hat{q}_0 = 2.0 \text{ GeV}^2/\text{fm}$ are compared with CMS data.

[CMS Collaboration, S. Chatrchyan et al.; Phys. Rev. Lett. **109**, 022301 (2012).]

Numerical results vs. data

Comparison with RHIC data

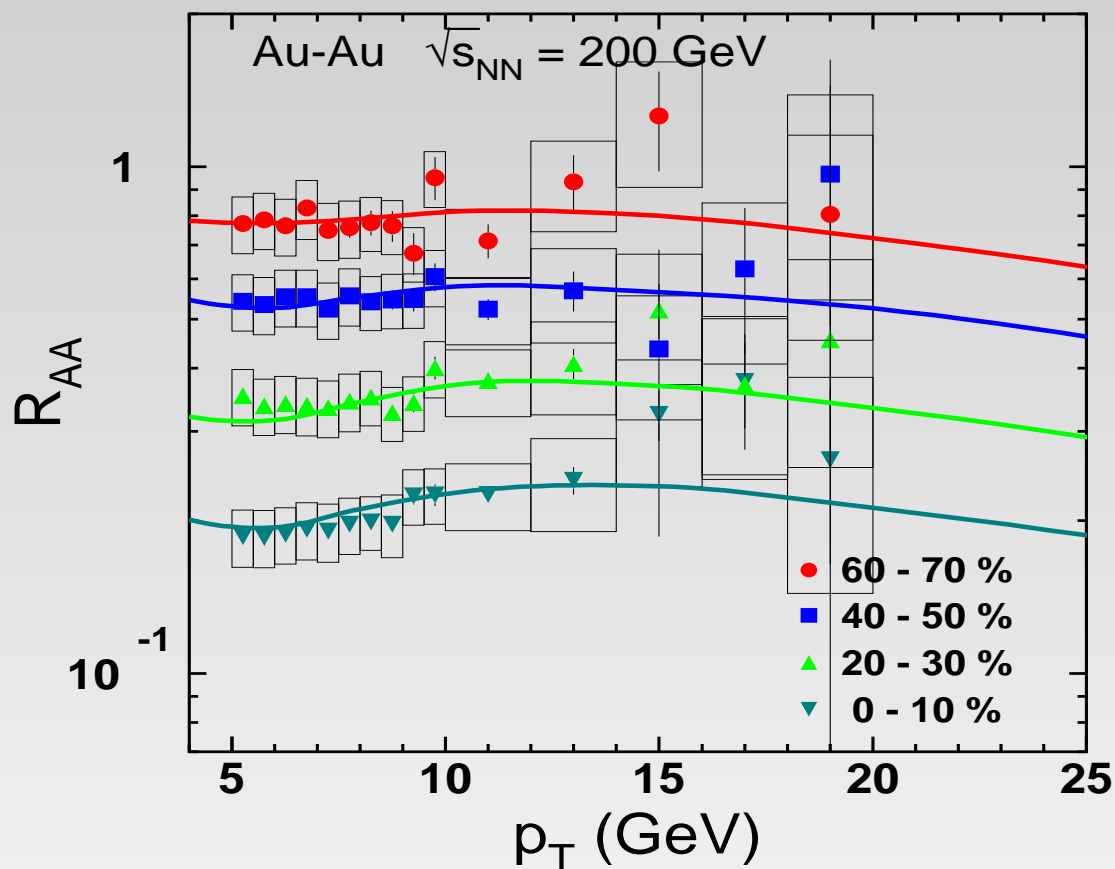


$R_{AA}(p_T)$ for neutral pions produced in central, 0-5%, gold-gold collisions at $\sqrt{s} = 200$ GeV. The GF calculations with $\hat{q}_0 = 1.6$ GeV²/fm are compared with PHENIX data.

[PHENIX Collaboration, A. Adare et al.; Phys. Rev. Lett. **101**, 232301 (2008); Phys. Rev. C **87**, 034911 (2013); M. L. Porschke et al.; J. Phys. G **38**, 124016 (2011).]

Numerical results vs. data

Comparison with RHIC data

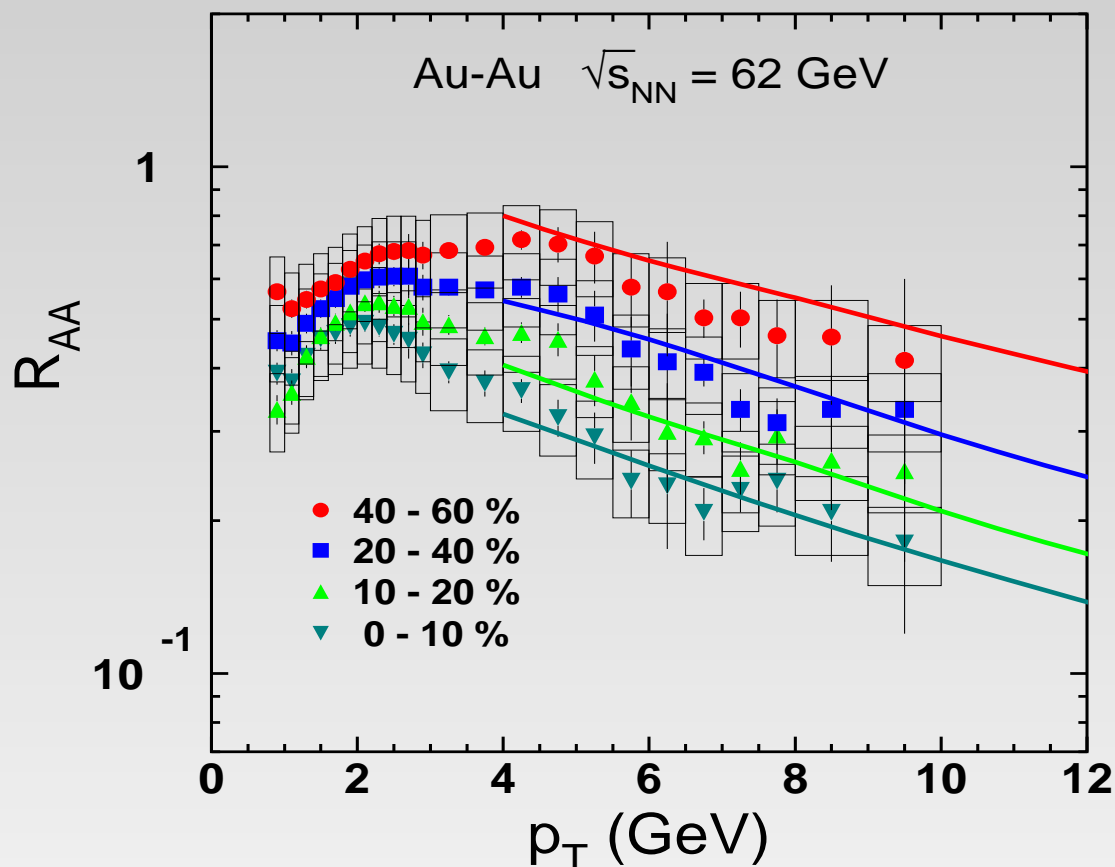


$R_{AA}(p_T)$ for neutral pions produced in Au-Au collisions at different centralities. The GF calculations with $\hat{q}_0 = 1.6$ GeV^2/fm are compared with PHENIX data.

[PHENIX Collaboration, A. Adare et al.; Phys. Rev. C87, 034911 (2013).]

Numerical results vs. data

Comparison with RHIC data

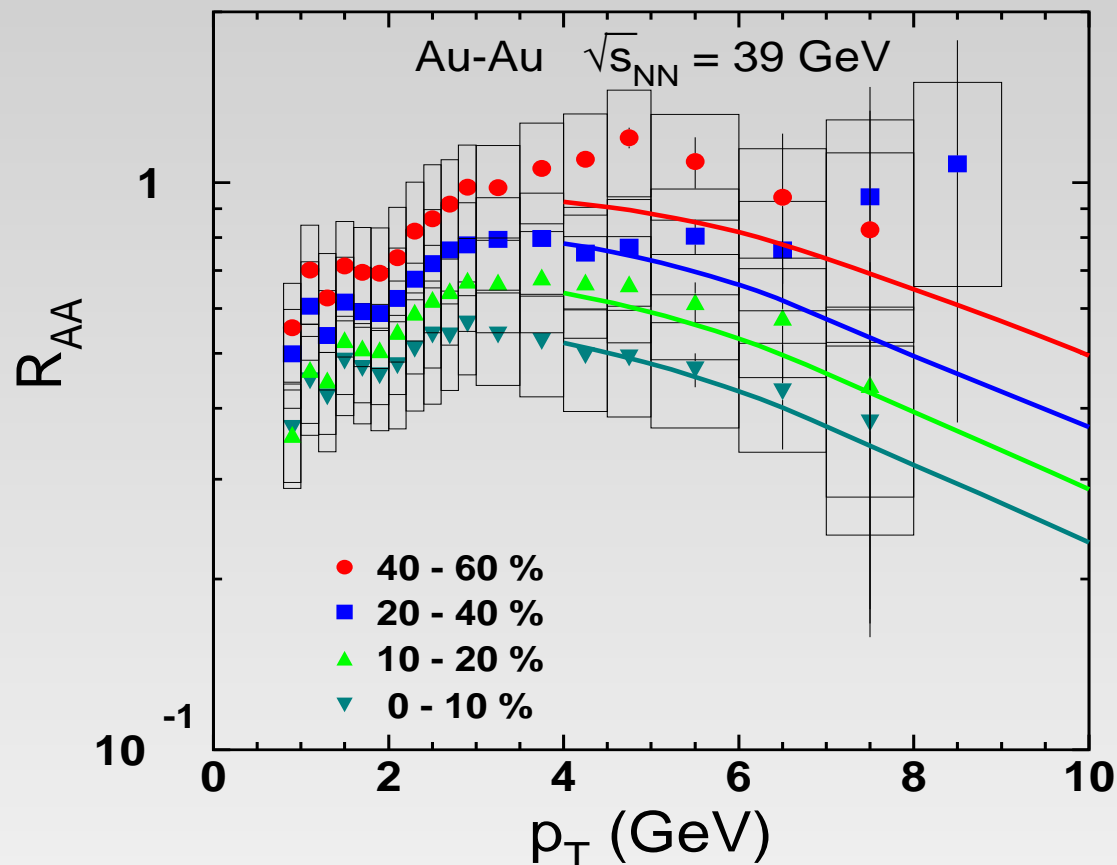


$R_{AA}(p_T)$ for neutral pions produced in gold-gold collisions at $\sqrt{s} = 62$ GeV and at different centralities. The GF calculations with $\hat{q}_0 = 1.2$ GeV²/fm are compared with PHENIX data. [PHENIX Collaboration, preliminary data posted at

http://www.phenix.bnl.gov/WWW/plots/show_plot.php?editkey=p1118]

Numerical results vs. data

Comparison with RHIC data

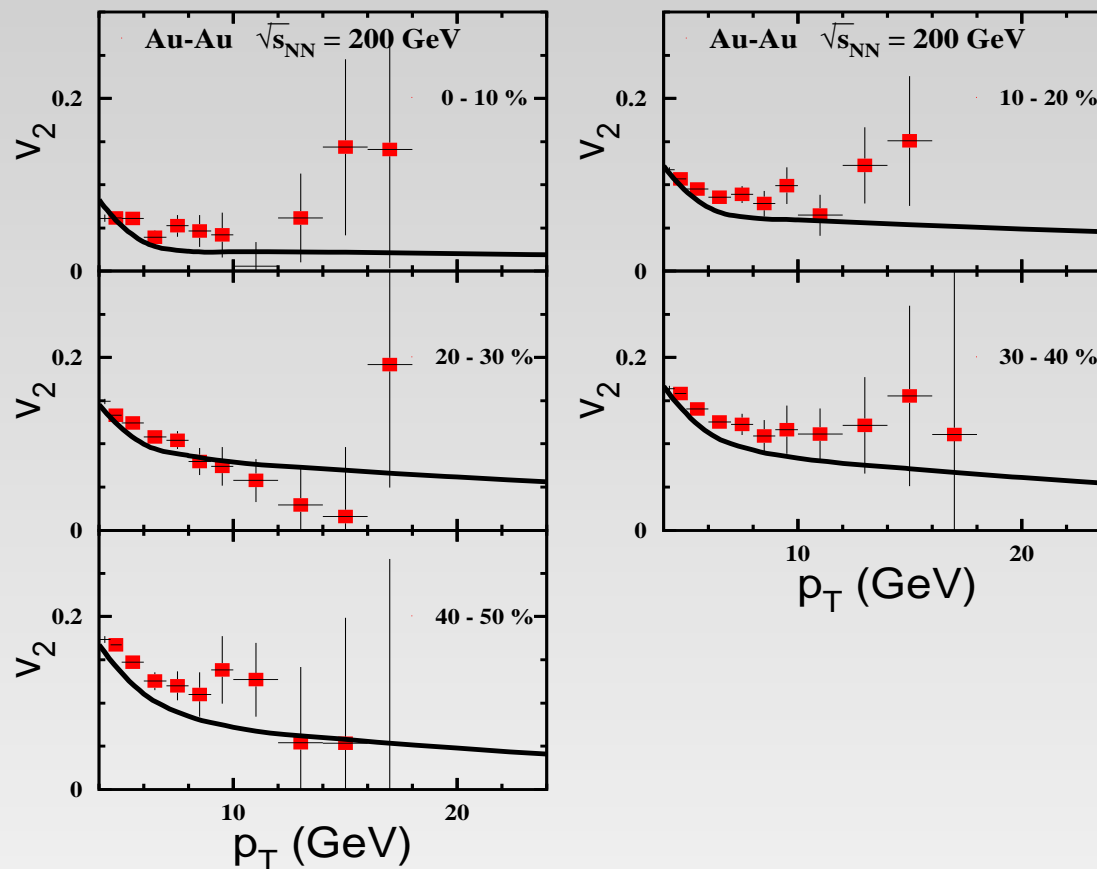


$R_{AA}(p_T)$ for neutral pions produced in gold-gold collisions at $\sqrt{s} = 39$ GeV and at different centralities. The GF calculations with $\hat{q}_0 = 0.6$ GeV²/fm are compared with PHENIX data. [PHENIX Collaboration, preliminary data posted at

http://www.phenix.bnl.gov/WWW/plots/show_plot.php?editkey=p1117]

Numerical results vs. data

Comparison with RHIC data - azimuthal asymmetry



Azimuthal anisotropy $v_2(p_T)$ for neutral pion production in gold-gold collisions at different centralities. The GF calculations with $\hat{q}_0 = 1.60 \text{ GeV}^2/\text{fm}$ are compared with PHENIX data.

[PHENIX Collaboration, A. Adare et al.; Phys. Rev. Lett. **105**, 142301 (2010).]

Numerical results vs. data

Hydrodynamics vs. pQCD

- Our pQCD calculations for $R_{AA}(p_T)$ and $v_2(p_T)$ grossly underestimate data at small $p_T \lesssim 6$ GeV.

Numerical results vs. data

Hydrodynamics vs. pQCD

- Our pQCD calculations for $R_{AA}(p_T)$ and $v_2(p_T)$ grossly underestimate data at small $p_T \lesssim 6$ GeV.
- The observed $R_{AA}(p_T)$ and $v_2(p_T)$ expose quite a different behavior towards smaller p_T , steeply rising and shaping a bump.

Numerical results vs. data

Hydrodynamics vs. pQCD

- Our pQCD calculations for $R_{AA}(p_T)$ and $v_2(p_T)$ grossly underestimate data at small $p_T \lesssim 6$ GeV.
- The observed $R_{AA}(p_T)$ and $v_2(p_T)$ expose quite a different behavior towards smaller p_T , steeply rising and shaping a bump.
- We relate this to an interplay of two mechanisms of hadron production: (i) evaporation of hadrons from the created hot medium controlled by hydrodynamics; (ii) perturbative QCD mechanism of high- p_T production of hadrons, which propagate and attenuate in the hot medium.

Numerical results vs. data

Hydrodynamics vs. pQCD

- Our pQCD calculations for $R_{AA}(p_T)$ and $v_2(p_T)$ grossly underestimate data at small $p_T \lesssim 6$ GeV.
- The observed $R_{AA}(p_T)$ and $v_2(p_T)$ expose quite a different behavior towards smaller p_T , steeply rising and shaping a bump.
- We relate this to an interplay of two mechanisms of hadron production: (i) evaporation of hadrons from the created hot medium controlled by hydrodynamics; (ii) perturbative QCD mechanism of high- p_T production of hadrons, which propagate and attenuate in the hot medium.
- The abrupt transition between the two mechanisms causes distinct minima in $R_{AA}(p_T)$ and in $v_2(p_T)$ both observed at the same values of p_T .

Numerical results vs. data

Hydrodynamics vs. pQCD

- Data on $R_{AA}(p_T)$ corresponding to In-plane and Out-of-plane events show that the transition from the hydrodynamic to perturbative regimes occur for In-plane events with a delay, at higher $p_T \Rightarrow$ the hydrodynamic flow is much stronger, correspondingly the cross section is larger.

Numerical results vs. data

Hydrodynamics vs. pQCD

- we combined our pQCD mechanism with hydrodynamic model from:

[Iu.A. Karpenko, Yu.M. Sinyukov, K. Werner; Phys. Rev. C87, 024914 (2013).]

Numerical results vs. data

Hydrodynamics vs. pQCD

- we combined our pQCD mechanism with hydrodynamic model from:
- [Iu.A. Karpenko, Yu.M. Sinyukov, K. Werner; Phys. Rev. C87, 024914 (2013).]

$$R_{AA}(p_T) = R_{AA}(p_T)_{hydro} + R_{AA}(p_T)_{pQCD}$$

Numerical results vs. data

Hydrodynamics vs. pQCD

- we combined our pQCD mechanism with hydrodynamic model from:
- [Iu.A. Karpenko, Yu.M. Sinyukov, K. Werner; Phys. Rev. C87, 024914 (2013).]

$$R_{AA}(p_T) = R_{AA}(p_T)_{hydro} + R_{AA}(p_T)_{pQCD}$$

- $$v_2(p_T) = \frac{v_2(p_T)_{hydro} R_{AA}(p_T)_{hydro} + v_2(p_T)_{pQCD} R_{AA}(p_T)_{pQCD}}{R_{AA}(p_T)_{hydro} + R_{AA}(p_T)_{pQCD}}$$

Numerical results vs. data

Hydrodynamics vs. pQCD

- we combined our pQCD mechanism with hydrodynamic model from:
- [Iu.A. Karpenko, Yu.M. Sinyukov, K. Werner; Phys. Rev. C87, 024914 (2013).]

$$R_{AA}(p_T) = R_{AA}(p_T)_{hydro} + R_{AA}(p_T)_{pQCD}$$

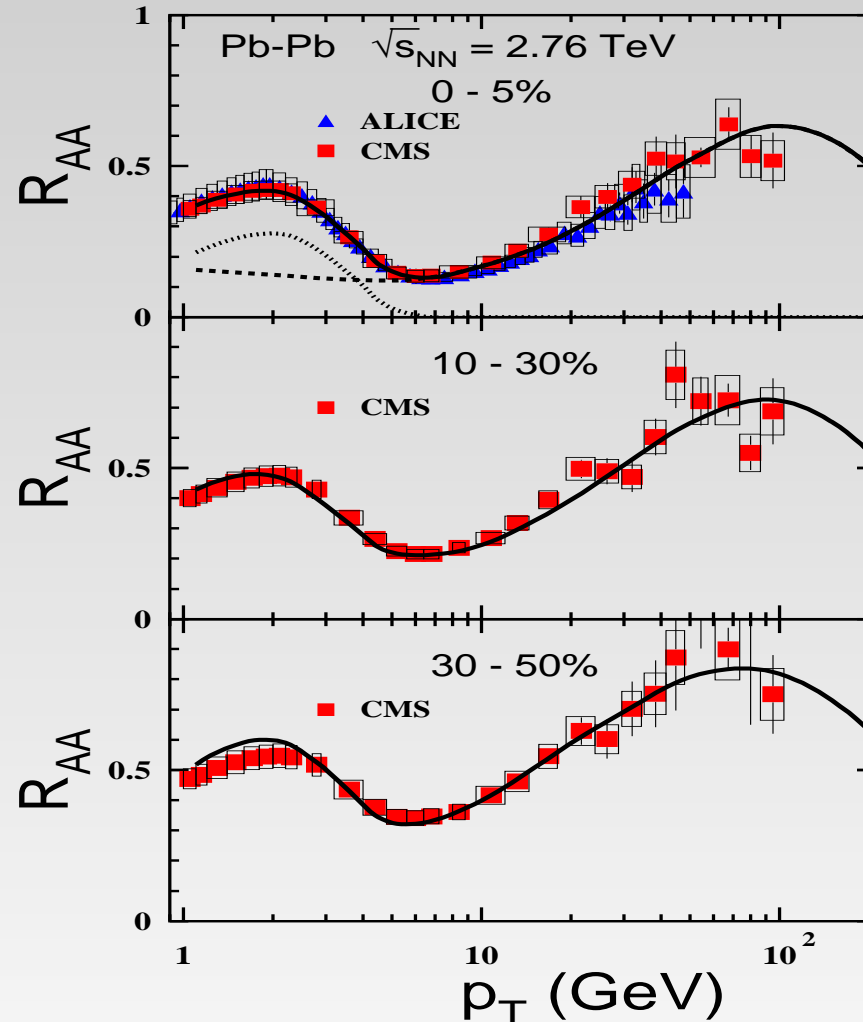
$$v_2(p_T) = \frac{v_2(p_T)_{hydro} R_{AA}(p_T)_{hydro} + v_2(p_T)_{pQCD} R_{AA}(p_T)_{pQCD}}{R_{AA}(p_T)_{hydro} + R_{AA}(p_T)_{pQCD}}$$

- where transverse momentum spectra of the hydrodynamic model are related to $R_{AA}(p_T)_{hydro}$ as:

$$R_{AA}(p_T)_{hydro} = \frac{d^2 N^{AA} / dy d^2 p_T [hydro]}{\langle T_{AA} \rangle d^2 \sigma_{pp} / dy d^2 p_T} f_p$$

Numerical results vs. data

Hydrodynamics vs. pQCD

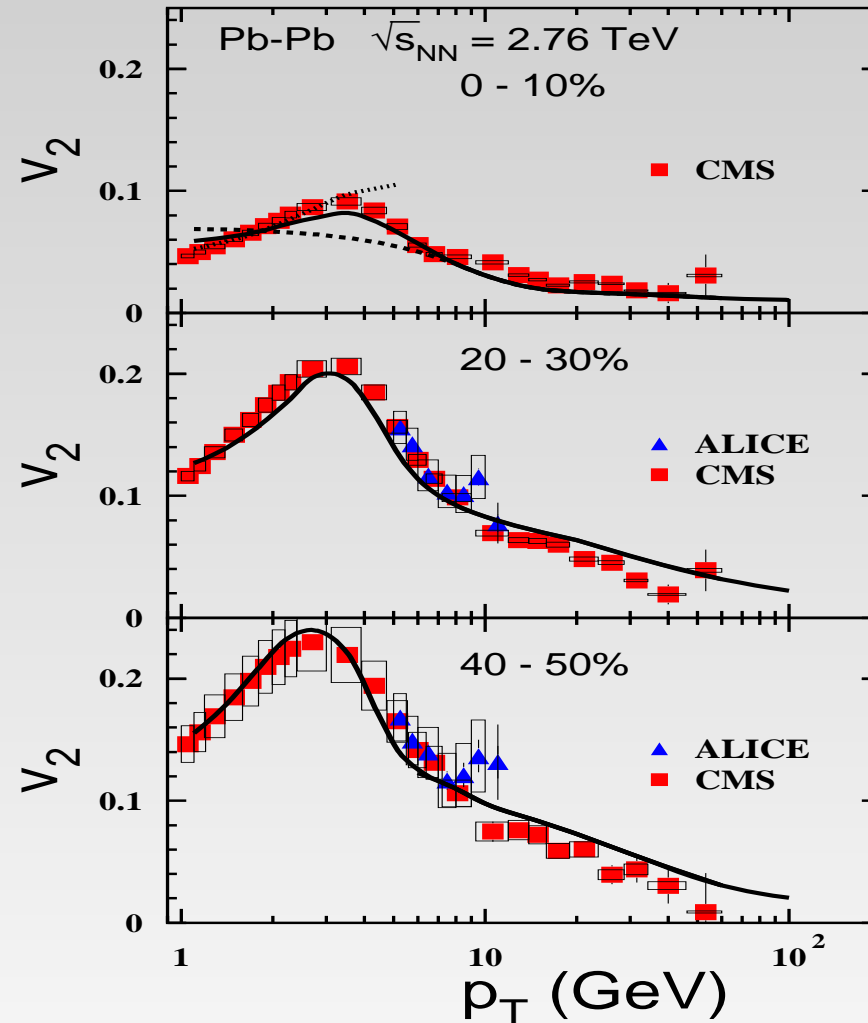


dotted line - nonperturbative HYDRO; dashed line - perturbative QCD

solid lines - combination of HYDRO and pQCD

Numerical results vs. data

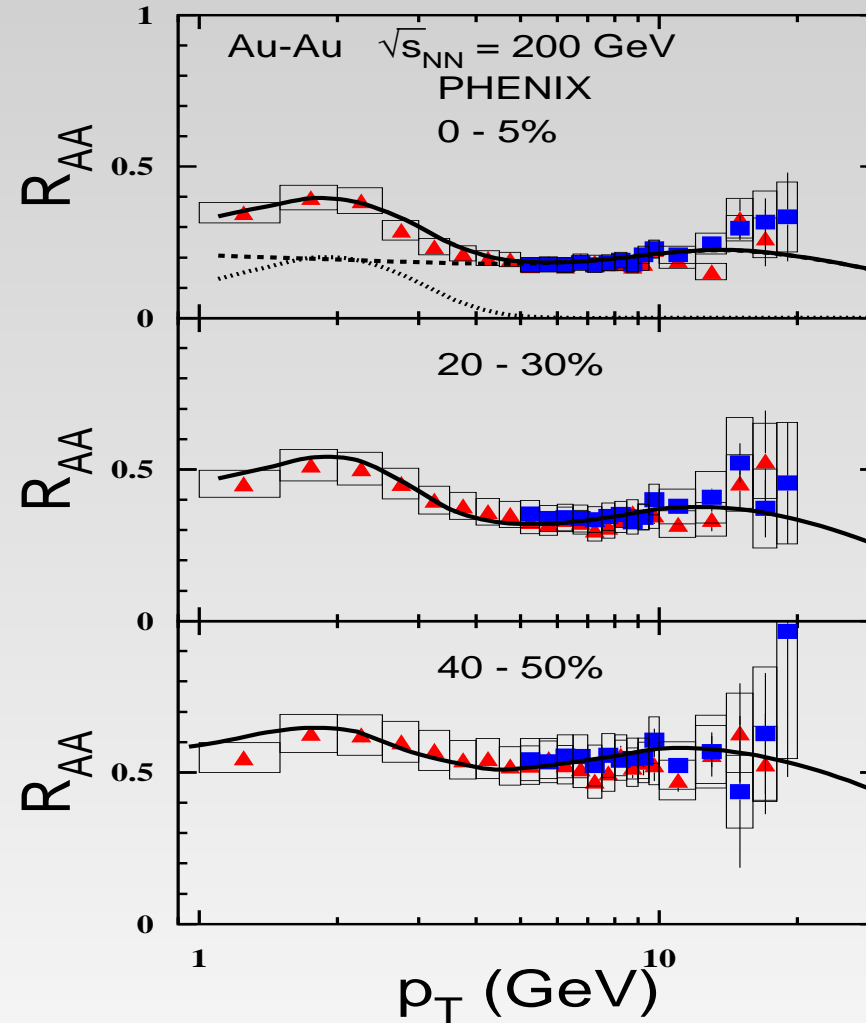
Hydrodynamics vs. pQCD



The dominant **hydrodynamic mechanism** of elliptic flow, provides a large and rising with p_T anisotropy $v_2(p_T)$, which abruptly switches to the **regime of pQCD**, having a much smaller azimuthal anisotropy.

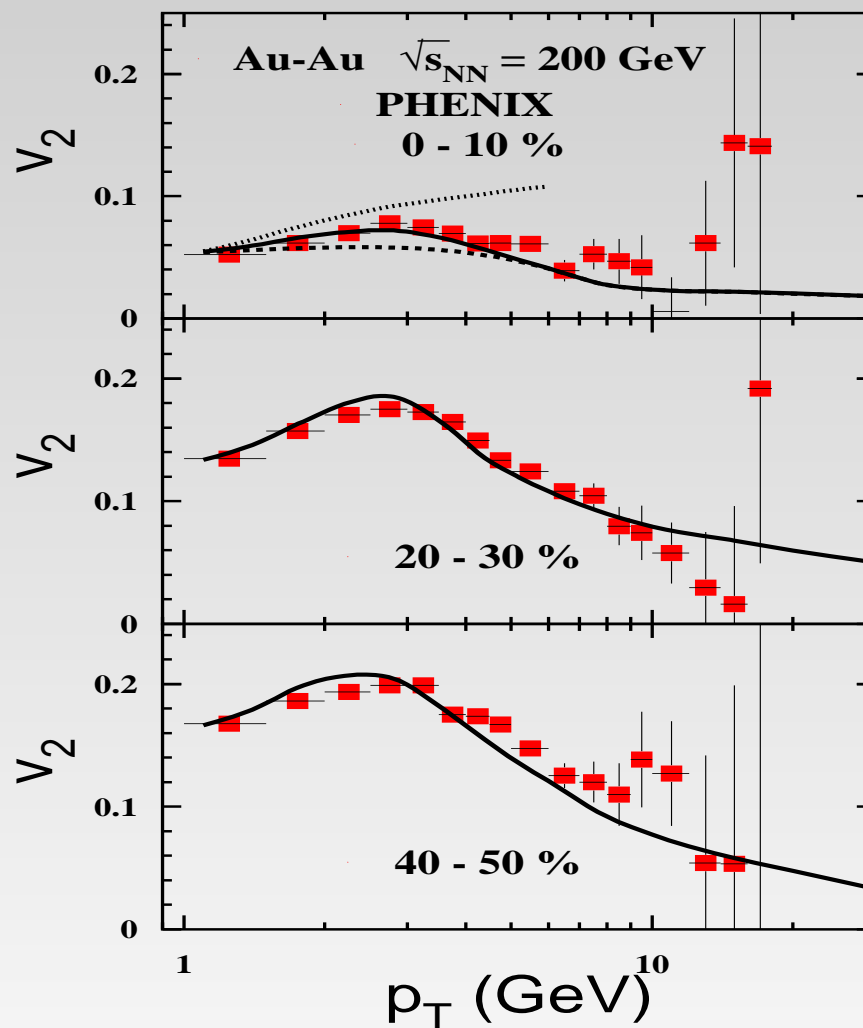
Numerical results vs. data

Hydrodynamics vs. pQCD



Numerical results vs. data

Hydrodynamics vs. pQCD



Summary

- Using the rigorous quantum-mechanical approach based on the path integral technique for description of the $\bar{q}q$ dipole evolution we apply the standard convolution expression for description of high- p_T hadron production in heavy ion collisions at mid rapidities in the RHIC and LHC kinematic range.

Summary

- Using the rigorous quantum-mechanical approach based on the path integral technique for description of the $\bar{q}q$ dipole evolution we apply the standard convolution expression for description of high- p_T hadron production in heavy ion collisions at mid rapidities in the RHIC and LHC kinematic range.
- The dynamics of a strong nuclear suppression of high- p_T hadrons is based on the **shortness of the production length**, l_p , of a colorless pre-hadrons and on its development and propagation through a dense medium.

Summary

- Using the rigorous quantum-mechanical approach based on the path integral technique for description of the $\bar{q}q$ dipole evolution we apply the standard convolution expression for description of high- p_T hadron production in heavy ion collisions at mid rapidities in the RHIC and LHC kinematic range.
- The dynamics of a strong nuclear suppression of high- p_T hadrons is based on the **shortness of the production length**, l_p , of a colorless pre-hadrons and on its development and propagation through a dense medium.
- the main part of nuclear suppression is related to the survival probability of colorless dipole propagating through a dense medium \Rightarrow **color transparency** - steep rise of the nuclear modification factor $R_{AA}(p_T)$ with p_T

Summary

- Using the rigorous quantum-mechanical approach based on the path integral technique for description of the $\bar{q}q$ dipole evolution we apply the standard convolution expression for description of high- p_T hadron production in heavy ion collisions at mid rapidities in the RHIC and LHC kinematic range.
- The dynamics of a strong nuclear suppression of high- p_T hadrons is based on the **shortness of the production length**, l_p , of a colorless pre-hadrons and on its development and propagation through a dense medium.
- the main part of nuclear suppression is related to the survival probability of colorless dipole propagating through a dense medium \Rightarrow **color transparency** - steep rise of the nuclear modification factor $R_{AA}(p_T)$ with p_T
- In comparison with LHC a dominance of quarks with larger l_p leads to a smaller suppression at RHIC.

Summary

- In the RHIC kinematic range we introduced also a suppression factor related to the constraints on nuclear parton distributions imposed by energy conservation.

Summary

- In the RHIC kinematic range we introduced also a suppression factor related to the constraints on nuclear parton distributions imposed by energy conservation.
- This suppression factor falling steeply with p_T is irrelevant at LHC but causes rather flat p_T dependence of R_{AA} at RHIC.

Summary

- In the RHIC kinematic range we introduced also a suppression factor related to the constraints on nuclear parton distributions imposed by energy conservation.
- This suppression factor falling steeply with p_T is irrelevant at LHC but causes rather flat p_T dependence of R_{AA} at RHIC.
- Calculations contain only medium density adjustment and we found the transport coefficient to be:

$$\hat{q}_0 = 0.60 \text{ GeV}^2 / \text{fm} \text{ at } \sqrt{s} = 39 \text{ GeV},$$

$$\hat{q}_0 = 1.20 \text{ GeV}^2 / \text{fm} \text{ at } \sqrt{s} = 62 \text{ GeV},$$

$$\hat{q}_0 = 1.60 \text{ GeV}^2 / \text{fm} \text{ at } \sqrt{s} = 200 \text{ GeV},$$

$$\hat{q}_0 = 2.00 \text{ GeV}^2 / \text{fm} \text{ at } \sqrt{s} = 2.76 \text{ TeV}.$$

Summary

- In the RHIC kinematic range we introduced also a suppression factor related to the constraints on nuclear parton distributions imposed by energy conservation.
- This suppression factor falling steeply with p_T is irrelevant at LHC but causes rather flat p_T dependence of R_{AA} at RHIC.
- Calculations contain only medium density adjustment and we found the transport coefficient to be:
 - $\hat{q}_0 = 0.60 \text{ GeV}^2 / \text{fm}$ at $\sqrt{s} = 39 \text{ GeV}$,
 - $\hat{q}_0 = 1.20 \text{ GeV}^2 / \text{fm}$ at $\sqrt{s} = 62 \text{ GeV}$,
 - $\hat{q}_0 = 1.60 \text{ GeV}^2 / \text{fm}$ at $\sqrt{s} = 200 \text{ GeV}$,
 - $\hat{q}_0 = 2.00 \text{ GeV}^2 / \text{fm}$ at $\sqrt{s} = 2.76 \text{ TeV}$.
- these value are more than order of magnitude less than was found from jet quenching data within the energy loss scenario

Summary

- In the RHIC kinematic range we introduced also a suppression factor related to the constraints on nuclear parton distributions imposed by energy conservation.
- This suppression factor falling steeply with p_T is irrelevant at LHC but causes rather flat p_T dependence of R_{AA} at RHIC.
- Calculations contain only medium density adjustment and we found the transport coefficient to be:
 - $\hat{q}_0 = 0.60 \text{ GeV}^2 / \text{fm}$ at $\sqrt{s} = 39 \text{ GeV}$,
 - $\hat{q}_0 = 1.20 \text{ GeV}^2 / \text{fm}$ at $\sqrt{s} = 62 \text{ GeV}$,
 - $\hat{q}_0 = 1.60 \text{ GeV}^2 / \text{fm}$ at $\sqrt{s} = 200 \text{ GeV}$,
 - $\hat{q}_0 = 2.00 \text{ GeV}^2 / \text{fm}$ at $\sqrt{s} = 2.76 \text{ TeV}$.
- these value are more than order of magnitude less than was found from jet quenching data within the energy loss scenario
- Finally we combined our pQCD results with the hydrodynamic mechanism providing a successful description of data in the full range of p_T .